

known, the genetic variations and linkage disequilibrium patterns reported in this study should be useful in the investigation of the genetic associations between *WFS1* and various diseases, especially in Japanese.

Acknowledgments

This study was supported by Grants-in-Aid for Scientific Research A–C, and for Scientific Research on Priority Areas (C) “Medical Genome Science” from the Japanese Ministry of Science, Education, Sports, Culture and Technology; for a Health and Labor Science Research Grant for Special Research from the Japanese Ministry of Health, Labor and Welfare; and for the Yamanouchi Foundation for Research on Metabolic Disorders, and Takeda Science Foundation.

References

- [1] D.J. Wolfram, H.P. Wagener, Diabetes mellitus and simple optic atrophy among siblings: report of four cases, *Mayo Clin. Proc.* 13 (1938) 715–718.
- [2] R.G. Swift, D.B. Sadler, M. Swift, Psychiatric findings in Wolfram syndrome homozygotes, *Lancet* 336 (1990) 667–669.
- [3] M.H. Polymeropoulos, R.G. Swift, M. Swift, Linkage of the gene for Wolfram syndrome to markers on the short arm of chromosome 4, *Nat. Genet.* 8 (1994) 95–97.
- [4] D.A. Collier, T.G. Barrett, D. Curtis, A. Macleod, M.J. Arranz, J.A. Maassen, S. Bunday, Linkage of Wolfram syndrome to chromosome 4p16.1 and evidence for heterogeneity, *Am. J. Hum. Genet.* 59 (1996) 855–863.
- [5] S. Nanko, H. Yokoyama, Y. Hoshino, H. Kumashiro, M. Mikuni, Organic mood syndrome in two siblings with Wolfram syndrome, *Br. J. Psychiatry* 16 (1992) 282.
- [6] H. Inoue, Y. Tanizawa, J. Wasson, P. Behn, K. Kalidas, E. Bernal-Mizrachi, M. Mueckler, H. Marshall, H. Donis-Keller, P. Crock, D. Rogers, M. Mikuni, H. Kumashiro, K. Higashi, G. Sobue, Y. Oka, M.A. Permutt, A gene encoding a transmembrane protein is mutated in patients with diabetes mellitus and optic atrophy (Wolfram syndrome), *Nat. Genet.* 20 (1998) 143–148.
- [7] T.M. Strom, K. Hortnagel, S. Hofmann, F. Gekeler, C. Scharfe, W. Rabl, K.D. Gerbitz, T. Meitinger, Diabetes insipidus, diabetes mellitus, optic atrophy and deafness (DIDMOAD) caused by mutations in a novel gene (wolframin) coding for a predicted transmembrane protein, *Hum. Mol. Genet.* 7 (1998) 2021–2028.
- [8] K. Takeda, H. Inoue, Y. Tanizawa, Y. Matsuzaki, J. Oba, Y. Watanabe, K. Shinoda, Y. Oka, *WFS1* (Wolfram syndrome 1) gene product: predominant subcellular localization to endoplasmic reticulum in cultured cells and neuronal expression in rat brain, *Hum. Mol. Genet.* 10 (2001) 477–484.
- [9] T.G. Barrett, S.E. Bunday, A.F. Macleod, Neurodegeneration and diabetes: UK nationwide study of Wolfram (DIDMOAD) syndrome, *Lancet* 346 (1995) 1458–1463.
- [10] A. Karasik, C. O’Hara, S. Srikanta, M. Swift, J.S. Soeldner, C.R. Kahn, R.D. Herskowitz, Genetically programmed selective islet beta-cell loss in diabetic subjects with Wolfram’s syndrome, *Diabetes Care* 12 (1989) 135–138.
- [11] R.G. Swift, M.H. Polymeropoulos, R. Torres, M. Swift, Predisposition of Wolfram syndrome heterozygotes to psychiatric illness, *Mol. Psychiatry* 3 (1998) 86–91.
- [12] D.H. Blackwood, L. He, S.W. Morris, A. McLean, C. Whitton, M. Thomson, M.T. Walker, K. Woodburn, C.M. Sharp, A.F. Wright, Y. Shibasaki, D.M. St Clair, D.J. Porteous, W.J. Muir, A locus for bipolar affective disorder on chromosome 4p, *Nat. Genet.* 12 (1996) 427–430.
- [13] P. Asherson, R. Mant, N. Williams, A. Cardno, L. Jones, K. Murphy, D.A. Collier, S. Nanko, N. Craddock, S. Morris, W. Muir, B. Blackwood, P. McGuffin, M.J. Owen, A study of chromosome 4p markers and dopamine D5 receptor gene in schizophrenia and bipolar disorder, *Mol. Psychiatry* 3 (1998) 310–320.
- [14] J.L. Kennedy, F.M. Macciardi, Chromosome 4 workshop, *Psychiatric Genet.* 8 (1998) 67–71.
- [15] F.H. Kooy, Hyperglycemia in mental disorders, *Brain* 42 (1919) 214–289.
- [16] S.L. Lilliker, Prevalence of diabetes in a manic-depressive population, *Compr. Psychiatry* 21 (1980) 270–275.
- [17] J.A. Gavard, P.J. Lustman, R.E. Clouse, Prevalence of depression in adults with diabetes. An epidemiological evaluation, *Diabetes Care* 16 (1993) 1167–1178.
- [18] F. Cassidy, E. Ahearn, B.J. Carroll, Elevated frequency of diabetes mellitus in hospitalized manic-depressive patients, *Am. J. Psychiatry* 156 (1999) 1417–1420.
- [19] W.T. Regenold, R.K. Thapar, C. Marano, S. Gavirneni, P.V. Kondapavuluru, Prevalence of type 2 diabetes mellitus among psychiatric inpatients with bipolar I affective and schizoaffective disorders independent of psychotropic drug use, *J. Affect. Disord.* 70 (2002) 19–26.
- [20] APA, Diagnostic and Statistical Manual of Mental Disorders, 4th DSM-IV ed. Washington, DC: American Psychiatric Press, 1994.
- [21] K. Cryns, T.A. Sivakumaran, J.M.W. Van den Ouweland, R.J.E. Pennings, C.W.R.J. Cremers, K. Flothmann, T.L. Young, R.J.H. Smith, M.M. Lesperance, G. Van Camp, Mutational spectrum of the *WFS1* gene in Wolfram syndrome, nonsyndromic hearing impairment, diabetes mellitus, and psychiatric disease, *Hum. Mutat.* 22 (2003) 275–287.
- [22] T. Awata, K. Inoue, S. Kurihara, T. Ohkubo, I. Inoue, T. Abe, H. Takino, Y. Kanazawa, S. Katayama, Missense variations of the gene responsible for Wolfram syndrome (*WFS1*/wolframin) in Japanese: possible contribution of the Arg456His mutation to type 1 diabetes as a nonautoimmune genetic basis, *Biochem. Biophys. Res. Commun.* 268 (2000) 612–616.
- [23] J.A. Minton, A.T. Hattersley, K. Owen, M.I. McCarthy, M. Walker, F. Latif, T. Barrett, T.M. Frayling, Association studies of genetic variation in the *WFS1* gene and type 2 diabetes in U.K. populations, *Diabetes* 51 (2002) 1287–1290.
- [24] T. Ohtsuki, H. Ishiguro, T. Yoshikawa, T. Arinami, *WFS1* gene mutation search in depressive patients: detection of five missense polymorphisms but no association with depression or bipolar affective disorder, *J. Affect. Disord.* 58 (2000) 11–17.
- [25] T. Kato, K. Iwamoto, S. Washizuka, K. Mori, O. Tajima, T. Akiyama, S. Nanko, H. Kunugi, N. Kato, No association of mutations and mRNA expression of *WFS1*/wolframin with bipolar disorder in humans, *Neurosci. Lett.* 338 (2003) 21–24.

Sex and age dependencies of cerebral blood volume changes during cognitive activation: a multichannel near-infrared spectroscopy study

Masaki Kameyama, Masato Fukuda,* Toru Uehara, and Masahiko Mikuni

Department of Psychiatry and Human Behavior, Gunma University Graduate School of Medicine, 3-39-22 Showa-machi, Maebashi, Gunma 371-8511, Japan

Received 30 December 2003; revised 23 March 2004; accepted 24 March 2004

In this study, we measured the change in cerebral hemoglobin concentrations during a cognitive task using multichannel near-infrared spectroscopy (NIRS), and investigated the relationship between regional cerebral blood volume and sex, age, and task performance. Thirty-nine healthy volunteers (24 males and 15 females; mean age, 33.0 years) participated after giving their informed consent and performed a word fluency task. The relative oxy-hemoglobin concentration ([oxy-Hb]) was measured using frontal and temporal probes with two sets of 24-channel NIRS machines. The effects of sex, age, and task performance on [oxy-Hb] changes were analyzed using analysis of covariance: with sex, age, and task performance as independent variables, and [oxy-Hb] changes as dependent variables, and years of education as covariates. The effects on [oxy-Hb] increase were significant in many channels in the frontal and temporal probes for sex, that is the most prominent effect, and in a few frontal channels for age: [oxy-Hb] increases were larger in males than in females, and in the young than in the middle-aged. The effects on [oxy-Hb] increase were not significant for task performance, but [oxy-Hb] increases in subjects with low performance tended to be larger than those in subjects with high performance. The results demonstrated that multichannel NIRS could detect cerebral activation during cognitive tasks and clarify sex- and age-dependent differences in such cerebral activation. Sex- and age-dependent differences in cerebral activation, as demonstrated in the present study, should be considered when interpreting cerebral blood volume, cerebral blood flow, and cerebral glucose metabolism data.

© 2004 Elsevier Inc. All rights reserved.

Keywords: Near-infrared spectroscopy; Cerebral blood volume; Sex differences; Aging; Performance; Word fluency test

Introduction

Recent advances in neuroimaging methodologies have enabled their application to the assessment of cognitive brain function in healthy subjects and diagnostic examination of neurological and psychiatric disorders. In interpreting obtained results, effects of

demographic parameters such as sex and age should be incorporated in data analyses.

A number of neuroimaging studies investigated the effects of sex and age on cognitive brain function. The greater lateralization of brain activation in males than in females was reported in language tasks using functional magnetic resonance imaging (fMRI) (Shaywitz et al., 1995; Vikingstad et al., 2000) and positron emission tomography (PET) (Jaeger et al., 1998). An age-dependent decline of brain activation was also well reported in cognitive tasks such as a calculation task (NIRS) (Hock et al., 1995), WAIS-III (NIRS and fMRI) (Kwee and Nakada, 2003), and a color-word-stroop task (NIRS) (Schroeter et al., 2003).

The effects of sex and age on cognitive function could interact with the performance of the task employed. Sex and age dependencies of cognitive functions have been well established: females perform better in verbal tasks, whereas males excel in spatial tasks (Collins and Kimura, 1997; Halpern, 2000; Silverman et al., 1996); the elderly perform more poorly than younger subjects in various cognitive tasks (Grady and Craik, 2000). However, as far as the authors surveyed, sex and age effects on brain function in relation to their interaction with task performance have not been fully clarified. This can cause problems in the interpretation of sex and age effect results: sex- or age-related differences in brain function could be the direct effects of sex or age, or the indirect effects of different task performances due to sex and age.

Near-infrared spectroscopy (NIRS) is a recently developed neuroimaging methodology. Its noninvasiveness (Ito et al., 2000), portability, natural setting of examination, and low running cost have enabled the examination of male and female subjects over a wide age range, from infancy to old age while performing cognitive tasks. Therefore, the effects of sex, age, and task performance should be studied in more detail using NIRS data interpretation.

NIRS can detect changes in the concentration of cerebral blood hemoglobins, such as oxy-hemoglobin ([oxy-Hb]), deoxy-hemoglobin ([deoxy-Hb]) and total-hemoglobin ([total-Hb]), which is the sum of [oxy-Hb] and [deoxy-Hb]. The principle of NIRS is based on the modified Lambert-Beer Law stating that the absorption of near-infrared light by oxy- and deoxy-hemoglobin varies with wavelength. Both [oxy-Hb] increases and [deoxy-Hb] decreases in NIRS are interpreted to reflect cortical activation

* Corresponding author. Department of Psychiatry and Human Behavior, Gunma University Graduate School of Medicine, 3-39-22 Showa-machi, Maebashi, Gunma 371-8511, Japan. Fax: +81-27-220-8192.

E-mail address: ikdpsy@med.gunma-u.ac.jp (M. Fukuda).

Available online on ScienceDirect (www.sciencedirect.com.)

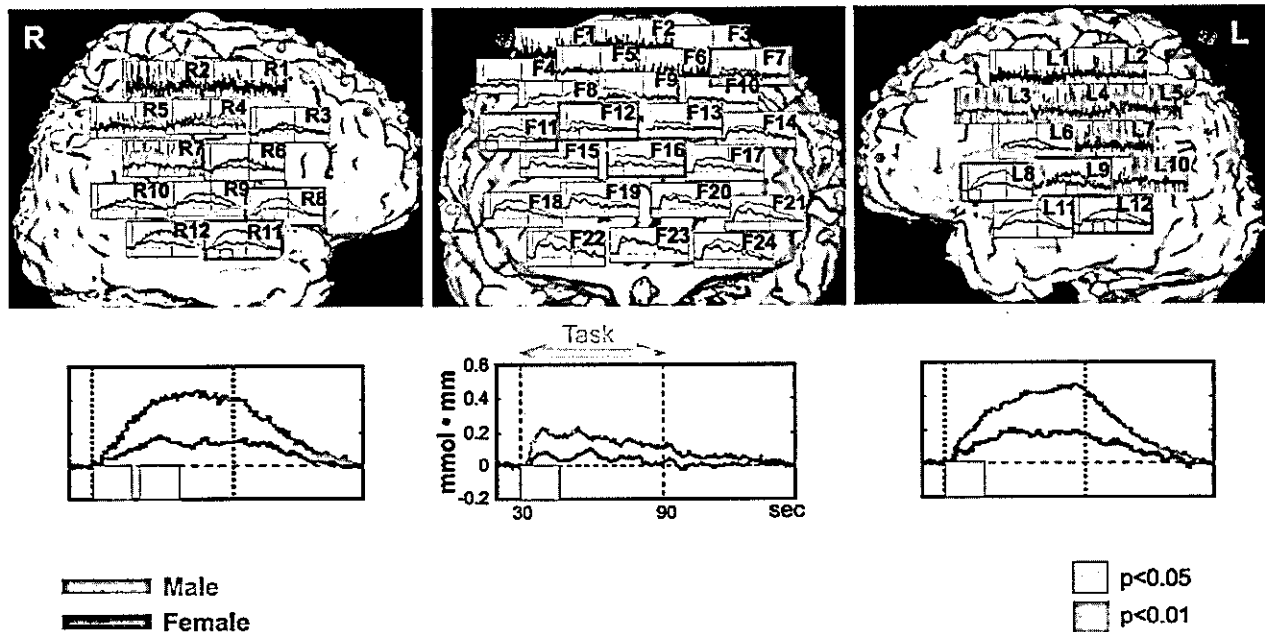


Fig. 1. Male group vs. female group. The upper figures show the grand average waveforms of oxy-hemoglobin changes obtained by NIRS in male (red line) and female subjects (blue line), superimposed on a reconstructed cerebral cortex image. The measurement channels with significant differences are displayed with thick red border lines and the time segments with significant differences in the channels are marked with red squares (filled squares, $P < 0.01$; unfilled squares, $P < 0.05$). Three representative channels (circled in yellow) are enlarged below.

because they have been shown to correspond to regional cerebral blood flow (CBF) in fMRI studies (Kleinschmidt et al., 1996; Toronov et al., 2001). Correlations of hemoglobin data in NIRS with CBF data simultaneously obtained using other methodologies have been shown to be stronger for [oxy-Hb] than for [deoxy-Hb] in a fMRI study (Strangman et al., 2002b) and a laser-Doppler study (Malonek et al., 1997). The differences are interpreted to be due to poorer contrast-to-noise ratios in the measurements of [deoxy-Hb] than in those of [oxy-Hb] (Strangman et al., 2002b). The technological principle of NIRS was reviewed in detail by Koizumi et al. (1999), Strangman et al. (2002a), and Obrig and Villringer (2003).

For human cognitive function, a number of NIRS studies have been published since 1993 (Chance et al., 1993; Hoshi and Tamura, 1993; Kato et al., 1993; Villringer et al., 1993) using various tasks: a confrontational writing task (Yamanoto et al., 1999), a speech listening task (Sato et al., 1999; Sakai et al., 2001), a calculation task (Hock et al., 1995), WAIS-III (Kwee and Nakada, 2003), and a word fluency (generation) task (Fallgatter et al., 1997; Herrmann et al., 2003; Hock et al., 1997; Matsuo et al., 2000, 2002; Suto et al., 2004; Watanabe et al., 1998). Some of these studies, using only one or two channels over a limited frontal area, investigated the effect of age, but not that of sex, on brain activation (Hock et al., 1995; Kwee and Nakada, 2003).

In the present study, we measured the changes in cerebral hemoglobin concentration using multichannel NIRS machines during a cognitive task, and investigated the relationship of regional cerebral blood volume (CBV) with sex, age, and task performance. The purpose of this study was to elucidate the effects of sex, age, and task performance on cerebral activation over larger brain areas along the task time course.

Materials and methods

Subjects

The subjects were 39 healthy volunteers (24 males and 15 females; mean age, 33.0 years; male mean age, 33.5 years ranging from 25 to 47; female mean age, 32.1 years ranging from 23 to 52; mean years of education, 16.8 years ranging from 12 to 22). Written informed consent was obtained from the subjects before the start of the investigation. All the subjects were right-handed as assessed by the Edinburgh Handedness Inventory (Oldfield, 1970). The handedness scores were mean 0.99, SD 0.05 for men and mean 0.96, SD 0.08 for women. None of the subjects had pre-existing neurological or psychiatric disorders. The present study was approved by the Institutional Review Board of Gunma University Graduate School of Medicine.

Task procedure

The subjects performed a word fluency task, which consisted of a 30-s pretask baseline period, a 60-s task period, and a 60-s post-task baseline period. The subjects were instructed in detail, in the instruction period before the NIRS measurements, to generate as many words as possible in the task period until they fully understood the task requirements. The initial syllables assigned were changed every 20 s (*ta*, *ka* and *sa*, respectively) during the 60-s task period. The words generated were monitored for correct and incorrect responses, and the number of correct words generated was determined as the subjects' task performance.

In the pretask and the post-task baseline periods, the subjects were instructed to repeat a train of syllables "*ta*, *ti*, *ta*, *te*, *to*". The subjects were seated in a comfortable chair with their eyes

open throughout the measurements. The timing of syllable changes was delivered to the subjects by the examiners' cue. The subjects were asked to avoid body movements such as neck movements, strong biting, and blinking during the NIRS measurements because they had been identified as most influential in the preliminary artifact-evoking study. The movements of the subjects were monitored throughout the examination.

NIRS measurements

NIRS machine

Relative [oxy-Hb], [deoxy-Hb], and [total-Hb] were measured with two sets of 24-channel NIRS machines (Hitachi ETG-100). The machine uses two wavelengths of the near-infrared light (780 and 830 nm), whose difference in the absorption spectrum enables the measurement of [oxy-Hb] and [deoxy-Hb] (Maki et al., 1995). The distance between pairs of emission and detector probes was set at 3.0 cm, which enabled cerebral blood volume measurements at a 2- to 3-cm depth from the skin of the head, that is, the surface of cerebral cortices (Hock et al., 1997; Toronov et al., 2001).

Probe positions and measurement points

The probes of the NIRS machines were fixed with thermoplastic shells and placed on the subject's frontal and bilateral temporal areas. The 16 probes on the subject's frontal area can measure the relative concentrations of hemoglobins at 24 measurement points in a 9×9 cm² area. The lowest probes in the frontal shell were positioned along the Fp₁–Fp₂ line according to the international 10/20 system used in electroencephalography. Each of the nine probes on the subject's bilateral temporal areas can measure the relative concentrations of hemoglobins at 12 measurement points in a 6×6 cm² area. The central probe in each temporal shell was positioned at the midpoint between the vertex and external ear hole. The measurement points were superimposed on a magnetic resonance image of a three-dimensionally reconstructed cerebral cortex of a subject. Measurement points were labeled as F1–F24 for the frontal channels, L1–L12 for the left temporal channels, and R1–R12 for the right temporal channels, from top to bottom.

Measurement parameters

The rate of data sampling was 0.1 s. Obtained data were analyzed using the "integral mode": the pretask baseline was determined as the mean over a 10-s period just before the task period, the post-task baseline was determined as the mean 5 s, 50 s after the task period, and linear fitting between the pre- and the post-task baselines was applied to data between the two baselines. The moving average method was adapted for analyzed data to remove short-term motion artifacts (moving average window: 1 s).

Data analyses

Data contaminated with artifacts due to body movements were excluded from further analyses. For data analyses, the task and the post-task periods were divided into six time segments along the time course: the task period into three segments ("task 1", "task 2", and "task 3" segments for the first, the second, and the third 20-s periods, respectively) and the post-task period into three segments ("post-task 1", "post-task 2", and "post-task 3" segments for the first 20-s, the second 20-s, and the third 15-s period, respectively). Obtained [oxy-Hb] data were averaged for each subject over these six time segments. Data from the channels

positioned over a hair-covered area often showed a low signal-to-noise ratio because of the paucity of near-infrared light detected, hence were excluded from the analyses when the standard deviations of [oxy-Hb] during the pretask period exceeded 0.035: four channels in the frontal shell (F1, F2, F3, and F6) and seven left channels (L1, L2, L3, L4, L5, L7, and L10) and five right channels (R1, R2, R4, R5, and R7) in the temporal shells.

For the remaining 32 channels with a sufficient signal-to-noise ratio, the effects of sex, age and task performance on [oxy-Hb] changes were analyzed over the six time segments using the three-way analysis of covariance (ANCOVA): with sex (24 males and 15 females), age (19 young and 20 middle-aged subjects, divided by the median age of the subjects, 29.0 years; the young group: mean age 26.3, SD 1.6 years; the middle-aged group: mean age 39.4, SD 6.7 years), and task performance (19 subjects with low performance and 20 subjects with high performance, divided by the median performance of 17 words) as independent variables, and [oxy-Hb] changes during the six time segments as dependent variables, and years of education as covariates. Statistical analysis was performed using SPSS 11.0J software (Tokyo, Japan).

In addition, the effects of the language nature of the task, which was employed in the present study, were examined for the left-right hemisphere asymmetry of [oxy-Hb] changes by comparing the channel pairs of mirror-imaged positions using a *t* test.

Results

The three-way ANCOVA demonstrated significant main effects of two independent variables, sex, and age (Table 1). Significant main effects of sex were obtained in four frontal channels (F7, F11, F12, F16) out of 20 channels analyzed, in three left temporal channels (L8, L9, L12) out of five channels analyzed, and two right temporal channels (R8 and R11) out of seven channels analyzed ($F = 4.4$ – 8.9 , $df = 1$, $P = 0.046$ – 0.006) (Fig. 1). In all the channels, [oxy-Hb] increases were larger in male than in female subjects. Time segments with significant differences were obtained only for task 1 in the frontal channels and from task 1 to task 3 in the temporal channels. Significant main effects of age were obtained only in four frontal channels (F11, F14, F15, F19) out of 20 channels analyzed ($F = 4.7$ – 6.2 , $df = 1$, $P = 0.037$ – 0.018) (Fig. 2). In these four channels, [oxy-Hb] increases were larger in the young than in the middle-aged subjects. The time segment with a significant difference in [oxy-Hb] changes was confined only to the task 1 segment. No significant main effect of task performance was obtained, but the mean [oxy-Hb] increases tended to be larger in the subjects with low performance than in the subjects with high performance in the two frontal (F19; post-task 1, F21; post-task 2), one left temporal (L9; post-task 1), and two right temporal (R3; task 1, R11; task 3) channels ($F = 2.9$ – 3.8 , $df = 1$, $P = 0.98$ – 0.062) (Fig. 3). Significant interactions among independent variables were obtained in two frontal and four temporal channels: the interaction of sex with age in the task 3 and post-task 1 segments in one frontal channel (F20; $F = 5.1$ and 4.9 , $df = 1$, $P = 0.032$ and 0.035 , respectively). The interaction of age with task performance in the task 1 and task 3 segments in one frontal channel (F5) and in the task 1 segment in one right temporal channel (R8; $F = 4.4$, $df = 1$, $P = 0.045$). The interaction of sex with task performance in one frontal (F5), one left (L9) and two right (R10 and R12) temporal channels ($F = 4.2$ – 6.5 , $df = 1$, $P = 0.048$ – 0.016) from task 1 to task 3 segments and the interaction of sex with age and task

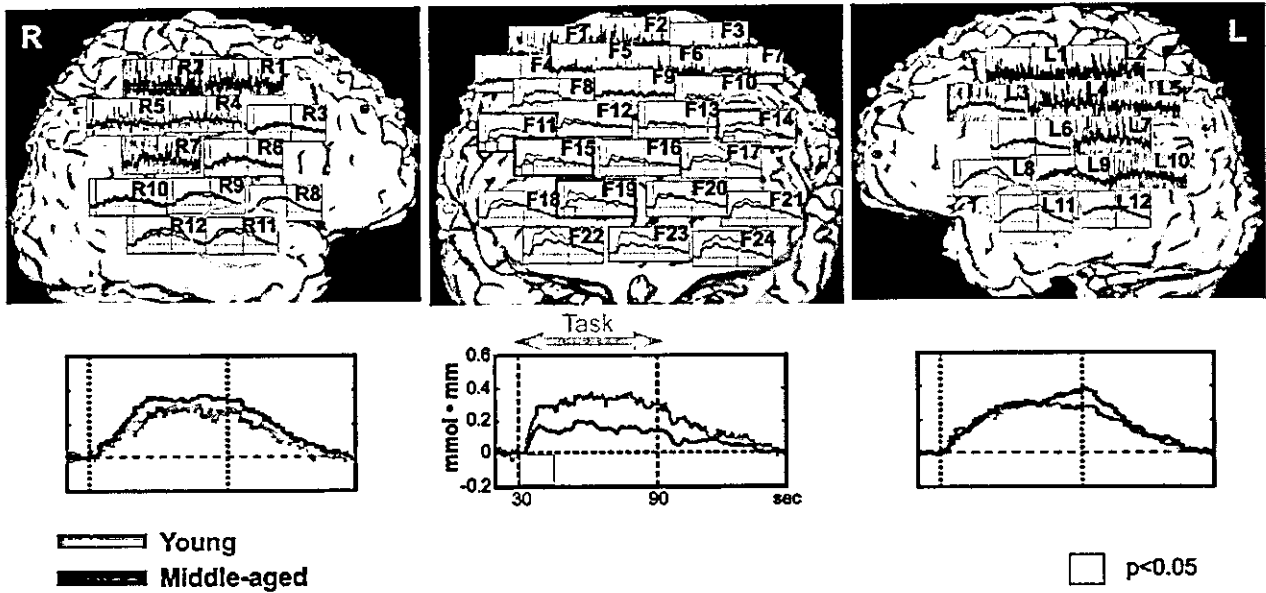


Fig. 2. Young group vs. middle-aged group. The upper figures show the grand average waveforms of oxy-hemoglobin changes obtained by NIRS in young (red line) and middle-aged subjects (blue line), superimposed on a reconstructed cerebral cortex image. The measurement channels with significant differences are displayed with thick red border lines and the time segments with significant differences in the channels are marked with red squares ($P < 0.05$). Three representative channels (circled in yellow) are enlarged below.

performance in the post-task 1 and post-task 2 segments in one right temporal channel (R8; $F = 5.0$ and 5.7 , $df = 1$, $P = 0.034$ and 0.023 , respectively). Covariate effects of the years of education were significant in eight frontal channels (F4, F5, F15, F18, F19,

F20, F21, F23) and three left (L8, L11, L12) and six right (R6, R8, R9, R10, R11, R12) temporal channels mainly in post-task period (from task 3 to post-task 3) for positive correlations with [oxy-Hb] increases ($F = 4.2–26.0$, $df = 1$, $P = 0.049–0.000$).

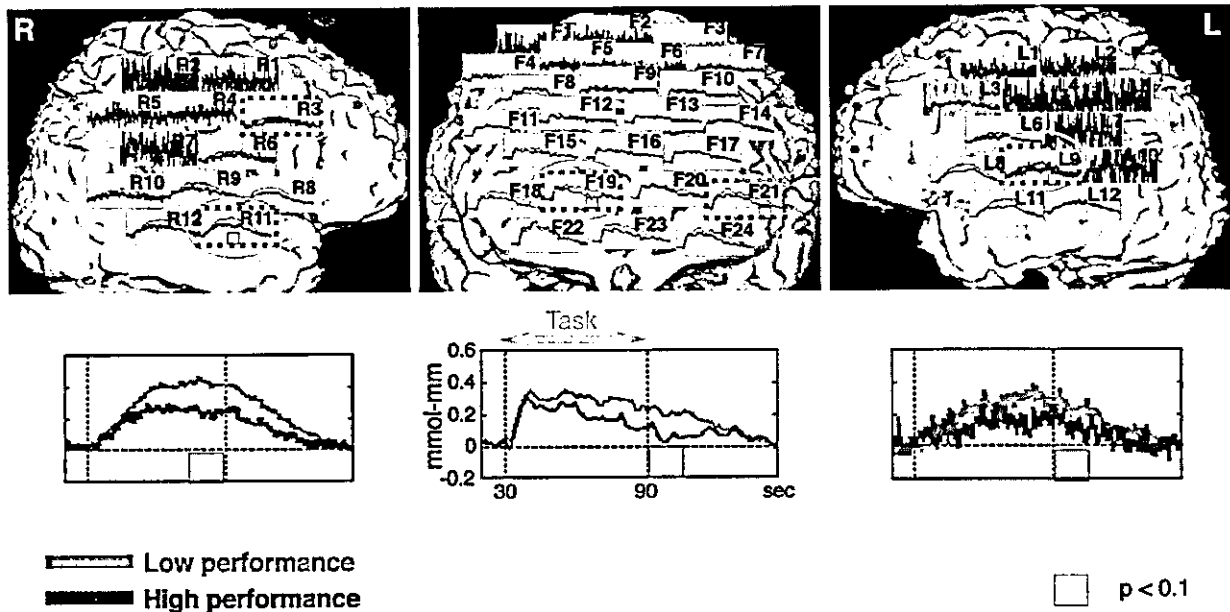


Fig. 3. Group with low performance vs. group with high performance. The upper figures show the grand average waveforms of oxy-hemoglobin changes obtained by NIRS in subjects with low performance (red line) and high performance (blue line), superimposed on a reconstructed cerebral cortex image. The measurement channels in which the mean [oxy-Hb] increases tended to be larger in the subjects with low performance than in the subjects with high performance are displayed with dotted red border lines and the time segments with differences in the channels are marked with red squares ($P < 0.1$). Three representative channels (circled in yellow) are enlarged below.

Table 1
Summary of the ANCOVA results for [oxy-Hb] changes

Channel	Time segment	Main effects			Interaction effects				Covariate
		sex (S)	age (A)	performance (P)	S × A	S × P	A × P	S × A × P	Education years
F5	task 1	1.9 (0.180)	2.5 (0.127)	0.2 (0.693)	0.2 (0.701)	4.4 (0.044)*	5.8 (0.023)*	1.5 (0.225)	1.7 (0.200)
	task 3	0.1 (0.784)	0.3 (0.603)	0.0 (0.996)	1.1 (0.292)	6.4 (0.017)*	5.1 (0.032)*	0.0 (0.937)	0.4 (0.526)
F7	task 1	8.9 (0.006)**	3.9 (0.059)	0.1 (0.733)	1.6 (0.215)	1.3 (0.263)	0.2 (0.655)	0.5 (0.480)	0.3 (0.592)
F11	task 1	5.0 (0.033)*	5.9 (0.022)*	0.1 (0.798)	1.5 (0.235)	0.6 (0.464)	0.4 (0.542)	0.0 (0.835)	0.1 (0.726)
F12	task 1	5.9 (0.021)*	3.3 (0.081)	1.5 (0.232)	1.9 (0.174)	1.2 (0.284)	0.1 (0.754)	0.5 (0.476)	0.0 (0.918)
F14	task 1	3.2 (0.083)	6.2 (0.018)*	0.2 (0.681)	0.2 (0.650)	0.1 (0.736)	0.1 (0.818)	0.0 (0.875)	0.6 (0.433)
F15	task 1	3.9 (0.058)	5.1 (0.031)*	0.1 (0.769)	0.4 (0.538)	0.9 (0.349)	0.0 (0.828)	0.0 (0.840)	0.0 (0.981)
F16	task 1	5.0 (0.033)*	3.0 (0.546)	0.1 (0.778)	2.3 (0.140)	0.1 (0.742)	0.0 (0.839)	0.1 (0.780)	0.0 (0.936)
F19	task 1	2.4 (0.133)	4.7 (0.037)*	0.2 (0.657)	0.2 (0.623)	0.0 (0.964)	0.3 (0.611)	0.1 (0.824)	0.1 (0.755)
F20	task 3	0.1 (0.724)	0.0 (0.898)	0.5 (0.498)	5.1 (0.032)*	1.3 (0.272)	0.9 (0.357)	0.2 (0.627)	1.5 (0.237)
	post-task 1	0.1 (0.802)	0.3 (0.586)	2.6 (0.116)	4.9 (0.035)*	0.1 (0.715)	0.4 (0.558)	0.1 (0.717)	1.7 (0.201)
L8	task 1	6.1 (0.020)*	0.0 (0.850)	0.6 (0.432)	0.0 (0.850)	0.9 (0.342)	0.0 (0.947)	0.0 (0.883)	0.1 (0.816)
L9	task 3	4.5 (0.043)*	0.1 (0.818)	2.6 (0.117)	0.7 (0.424)	4.3 (0.048)*	0.1 (0.741)	1.2 (0.288)	0.4 (0.550)
L12	task 2	4.4 (0.046)*	0.1 (0.706)	0.2 (0.655)	0.1 (0.742)	0.1 (0.750)	1.1 (0.292)	2.8 (0.104)	0.1 (0.966)
R8	task 1	4.4 (0.045)*	0.2 (0.630)	0.9 (0.348)	0.1 (0.777)	0.2 (0.660)	0.1 (0.809)	0.3 (0.566)	0.1 (0.817)
	task 2	4.8 (0.037)*	0.0 (0.986)	0.9 (0.345)	0.5 (0.466)	1.6 (0.212)	0.9 (0.339)	1.0 (0.337)	1.0 (0.328)
	post-task 1	1.4 (0.247)	0.2 (0.691)	0.9 (0.344)	0.5 (0.499)	2.5 (0.125)	4.4 (0.045)*	5.0 (0.034)*	13.3 (0.001)**
	post-task 2	0.0 (0.906)	1.3 (0.270)	2.0 (0.165)	0.1 (0.768)	0.6 (0.464)	3.3 (0.078)	5.7 (0.023)*	26.0 (0.000)**
R10	task 2	2.1 (0.156)	0.1 (0.760)	0.2 (0.649)	0.4 (0.527)	5.1 (0.031)*	0.0 (0.985)	1.3 (0.265)	0.1 (0.759)
	task 3	0.9 (0.343)	0.1 (0.815)	0.1 (0.709)	0.5 (0.480)	6.5 (0.016)*	1.1 (0.299)	0.8 (0.383)	2.9 (0.099)
R11	task 1	5.1 (0.031)*	0.0 (0.907)	0.6 (0.427)	0.1 (0.763)	0.3 (0.585)	1.3 (0.262)	0.0 (0.897)	0.2 (0.684)
	task 2	4.4 (0.045)*	0.2 (0.635)	1.5 (0.224)	0.1 (0.714)	2.7 (0.109)	2.9 (0.098)	0.3 (0.574)	3.6 (0.066)
R12	task 2	1.5 (0.228)	0.1 (0.753)	0.3 (0.575)	0.5 (0.490)	4.2 (0.048)*	0.5 (0.488)	0.6 (0.434)	2.9 (0.098)
	task 3	1.1 (0.302)	0.2 (0.645)	0.5 (0.480)	0.4 (0.510)	5.6 (0.024)*	1.3 (0.260)	0.6 (0.462)	7.2 (0.012)*

F and *P* values are shown only for the channels and time segments with statistical significance in main and interaction effects as '*F* (*P*)'.

**P* < 0.05.

***P* < 0.01.

All the *t* tests examining the left–right hemisphere asymmetry of [oxy-Hb] changes showed no significant differences.

Discussion

The present study examined the effects of sex, age, and task performance on brain activation during a cognitive task using multichannel NIRS. The statistically significant main effects on [oxy-Hb] increase were obtained for sex in many channels in the frontal and temporal probes and for age in a few frontal channels: [oxy-Hb] increases were larger in males than in females, and in the young than in the middle-aged. On the other hand, the main effect of task performance on [oxy-Hb] increases was not significant, although [oxy-Hb] increases in subjects with low performance tended to be larger than those in subjects with high performance.

The obtained differences in cerebral activation for sex during the cognitive task are consistent with a previous PET study by Buckner et al. (1995) that demonstrated a larger prefrontal activation in male than in female subjects during a verb generation task. They interpreted the result as being derived from the difference in difficulty performing the same task between male and female subjects based on the better performance of the female subjects: in general, female subjects perform language tasks more efficiently than male subjects (Halpern, 2000). However, this explanation is not relevant for the present study because the task performance was equal between the male and the female subjects.

The age-dependent decrease in cerebral activation during the cognitive task is consistent with previous NIRS studies using a calculation task (Hock et al., 1995), WAIS III (Kwee and Nakada,

2003), and a color-word-stroop task (Schroeter et al., 2003), and with a PET study using a serial verbal learning test (Hazlett et al., 1998). The authors of these previous reports assumed the decrease to be the consequence of structural cortical changes (decrease of region-specific cortical thickness and shrinkage of neuronal dendrites), functional cortical changes (decline of frontal activation), or the decline of working memory utilization due to aging. The rather low age range of the subjects in the present study (23–52 years old) and the absence of a significant difference in the task performance between the young and the middle-aged subjects could exclude the first and the third interpretations mentioned above, respectively.

Larger [oxy-Hb] increases in the subjects with high performance, although the differences did not reach statistical significance, are consistent with the findings of task performance dependencies of cerebral metabolism activation in a PET study using a verbal fluency test (Parks et al., 1988), and CBV changes in an NIRS study using the calculation task (Hoshi and Tamura, 1993). The finding could be interpreted as indicating greater effort and hence less efficient processing in poor performers.

As for the laterality of brain activation in the language task, previous brain imaging studies reported a left lateralized pattern with some inconsistencies: both in male and female subjects (Buckner et al., 1995; Frost et al., 1999; Schlosser et al., 1998) or only in male subjects (Shaywitz et al., 1995; Vikingstad et al., 2000). The absence of such a left lateralized pattern in the present study could be explained by the task characteristics employed. The change in [oxy-Hb] was determined as the difference between the syllable-repeating condition in the pretask baseline period and the word-fluency condition in the task period. Such a

measurement could result in subtracting the utterance process-related activation from the word generation-related activation, resulting in an altered lateralization of brain activation. In fact, orthographic, phonological, and semantic processing in language tasks were reported to be differentially lateralized in a fMRI study (Shaywitz et al., 1995).

The distinction between baseline CBF and activation-related changes in CBF and CBV should be stressed. The present study, as well as the studies mentioned above, examined activation-related changes in CBF and CBV using NIRS, PET, SPECT, and fMRI.

The effects of sex and age on baseline levels of CBF, CBV, and cerebral glucose metabolism measured at the resting state have been reported with rather different results from those of activation studies. Studies on sex differences in CBF, CBV, and cerebral glucose metabolism yielded variable results in the resting state as well as in the activation state. Compared with male subjects, cerebral perfusion and metabolism in female subjects were reported to be higher both in terms of global CBF (Gur et al., 1982; Rodriguez et al., 1988) and regional CBF in the temporal regions (Ragland et al., 2000), but to be lower in terms of cerebral glucose metabolism in the temporal-limbic region (Gur et al., 1995), and to be without significant difference in cerebral glucose metabolism (Azari et al., 1992). The results of these studies in the resting state should be taken into consideration when interpreting the results of activation studies: for example, increased baseline perfusion and metabolism could result in decreased activation due to the ceiling effect. However, as far as the authors surveyed, no studies that examined baseline and activation levels simultaneously in the same subjects have been carried out.

The age-dependent decrease in CBF, CBV, and cerebral glucose metabolism in the resting state as well as in the activation state, in contrast, has been frequently replicated (Marchal et al., 1992; Meltzer et al., 2000; Murphy et al., 1996; Pantano et al., 1984; Yamaguchi et al., 1986). The age-dependent decrease in cerebral perfusion and metabolism in the resting state is hypothesized to result from the combined effects of direct neuronal loss, cellular biological impairment, and functional deafferentation (Marchal et al., 1992) and such mechanisms could also underlie the age-dependent decrease in activation in terms of cerebral perfusion and metabolism.

Two limitations in the present study should be addressed. First, NIRS measures the hemoglobin concentration changes only as relative values. The estimation of hemoglobin concentration changes depends on the assumed near-infrared pathlength: hence, differences in this pathlength among the subjects could influence the obtained results. The result for age effect, at least, should be interpreted carefully because pathlength was reported to be weakly dependent on age, approximately 5% for 10 years at the most (Duncan et al., 1996), but not on sex (Duncan et al., 1995). Second, the NIRS probes employed in the present study covered only limited cerebral regions. We could not measure regional CBV over gap areas between the frontal and temporal probes as well as between the parietal and occipital areas, and the left gap area is assumed to correspond to Broca's area. Measurement of regional CBV in Broca's area could demonstrate different results regarding age, sex, and task performance dependencies. Further studies are required to address these limitations.

In conclusion, the present study demonstrated that multi-channel NIRS can detect cerebral activation during cognitive tasks and can also clarify sex- and age-dependent differences in

such cerebral activation. Sex- and age-dependent differences in cerebral activation obtained in the present study should be considered when interpreting CBF, CBV, and cerebral glucose metabolism data.

Acknowledgments

This research was supported in part by a grant-in-aid for Scientific Research (C) from the Japanese Ministry of Education, Culture, Sports, Science and Technology (MF), a Health and Labour Sciences Research Grant for Research on Psychiatric and Neurological Diseases and Mental Health (MF), and a Health and Labour Sciences Research Grant for Special Research from the Japanese Ministry of Health, Labour and Welfare (MM). The authors gratefully thank Drs. Itsuro Ida, Tomohiro Suto, Makoto Ito, and Yutaka Yamagishi of the Department of Psychiatry and Human Behavior, Gunma University Graduate School of Medicine and two medical students, Mr. Ryu Takizawa and Ms. Ayako Kawakami, of the same university for their collaborations. The authors also gratefully acknowledge the assistance of Mr. Suguru Hattori in statistical analysis.

References

- Azari, N.P., Rapoport, S.I., Grady, C.L., DeCarli, C., Haxby, J.V., Schapiro, M.B., et al., 1992. Gender differences in correlations of cerebral glucose metabolic rates in young normal adults. *Brain Res.* 574, 198–208.
- Buckner, R.L., Raichle, M.E., Petersen, S.E., 1995. Dissociation of human prefrontal cortical areas across different speech production tasks and gender groups. *J. Neurophysiol.* 74, 2163–2173.
- Chance, B., Zhuang, Z., UnAh, C., Alter, C., Lipton, L., 1993. Cognition-activated low-frequency modulation of light absorption in human brain. *Proc. Natl. Acad. Sci. U. S. A.* 90, 3770–3774.
- Collins, D.W., Kimura, D., 1997. A large sex difference on a two-dimensional mental rotation task. *Behav. Neurosci.* 111, 845–849.
- Duncan, A., Meek, J.H., Clemence, M., Elwell, C.E., Tyszczyk, L., Cope, M., et al., 1995. Optical pathlength measurements on adult head, calf and forearm and the head of the newborn infant using phase resolved optical spectroscopy. *Phys. Med. Biol.* 40, 295–304.
- Duncan, A., Meek, J.H., Clemence, M., Elwell, C.E., Fallon, P., Tyszczyk, L., et al., 1996. Measurement of cranial optical path length as a function of age using phase resolved near infrared spectroscopy. *Pediatr. Res.* 39, 889–894.
- Fallgatter, A.J., Roesler, M., Sitzmann, L., Heidrich, A., Mueller, T.J., Strik, W.K., 1997. Loss of functional hemispheric asymmetry in Alzheimer's dementia assessed with near-infrared spectroscopy. *Brain Res. Cogn. Brain Res.* 6, 67–72.
- Frost, J.A., Binder, J.R., Springer, J.A., Hanumake, T.A., Bellgowan, P.S., Rao, S.M., et al., 1999. Language processing is strongly left lateralized in both sexes. Evidence from functional MRI. *Brain* 122, 199–208.
- Grady, C.L., Craik, F.I., 2000. Changes in memory processing with age. *Curr. Opin. Neurobiol.* 10, 224–231.
- Gur, R.C., Gur, R.E., Obrist, W.D., Hungerbuhler, J.P., Younkin, D., Rosen, A.D., et al., 1982. Sex and handedness differences in cerebral blood flow during rest and cognitive activity. *Science* 217, 659–661.
- Gur, R.C., Mozley, L.H., Mozley, P.D., Resnick, S.M., Karp, J.S., Alavi, A., et al., 1995. Sex differences in regional cerebral glucose metabolism during a resting state. *Science* 267, 528–531.
- Halpern, D.F., 2000. Sex differences in cognitive abilities. third ed. Lawrence Erlbaum Associates, Mahwah, NJ.
- Hazlett, E.A., Buchsbaum, M.S., Mohs, R.C., Spiegel-Cohen, J., Wei, T.C.,

- Azueta, R., et al., 1998. Age-related shift in brain region activity during successful memory performance. *Neurobiol. Aging* 19, 437–445.
- Herrmann, M.J., Fblis, A.C., Fallgatter, A.J., 2003. Frontal activation during a verbal-fluency task as measured by near-infrared spectroscopy. *Brain Res. Bull.* 61, 51–56.
- Hock, C., Muller-Spahn, F., Schuh-Hofer, S., Hofmann, M., Dimagl, U., Villringer, A., 1995. Age dependency of changes in cerebral hemoglobin oxygenation during brain activation: a near-infrared spectroscopy study. *J. Cereb. Blood Flow Metab.* 15, 1103–1108.
- Hock, C., Villringer, K., Muller-Spahn, F., Wenzel, R., Heekeren, H., Schuh-Hofer, S., et al., 1997. Decrease in parietal cerebral hemoglobin oxygenation during performance of a verbal fluency task in patients with Alzheimer's disease monitored by means of near-infrared spectroscopy (NIRS): correlation with simultaneous rCBF-PET measurements. *Brain Res.* 755, 293–303.
- Hoshi, Y., Tamura, M., 1993. Detection of dynamic changes in cerebral oxygenation coupled to neuronal function during mental work in man. *Neurosci. Lett.* 150, 5–8.
- Ito, Y., Kanaan, R.P., Watanabe, E., Koizumi, H., 2000. Assessment of heating effects in skin during continuous wave near infrared spectroscopy. *J. Biomed. Opt.* 5, 383–390.
- Jaeger, J.J., Lockwood, A.H., Van Valin Jr., R.D., Kemmerer, D.L., Murphy, B.W., Wack, D.S., 1998. Sex differences in brain regions activated by grammatical and reading tasks. *NeuroReport* 9, 2803–2807.
- Kato, T., Kanei, A., Takashima, S., Ozaki, T., 1993. Human visual cortical function during photic stimulation monitoring by means of near-infrared spectroscopy. *J. Cereb. Blood Flow Metab.* 13, 516–520.
- Kleinschmidt, A., Obrig, H., Requardt, M., Merboldt, K.D., Dimagl, U., Villringer, A., et al., 1996. Simultaneous recording of cerebral blood oxygenation changes during human brain activation by magnetic resonance imaging and near-infrared spectroscopy. *J. Cereb. Blood Flow Metab.* 16, 817–826.
- Koizumi, H., Yamashita, Y., Maki, A., Yamamoto, T., Ito, Y., Itagaki, H., et al., 1999. Higher-order brain function analysis by trans-cranial dynamic near-infrared spectroscopy imaging. *J. Biomed. Opt.* 4, 403–413.
- Kwee, I.L., Nakada, T., 2003. Dorsolateral prefrontal lobe activation declines significantly with age: functional NIRS study. *J. Neurol.* 250, 525–529.
- Maki, A., Yamashita, Y., Ito, Y., Watanabe, E., Mayanagi, Y., Koizumi, H., 1995. Spatial and temporal analysis of human motor activity using noninvasive NIR topography. *Med. Phys.* 22, 1997–2005.
- Malonek, D., Dimagl, U., Lindauer, U., Yamada, K., Kanno, I., Grinvald, A., 1997. Vascular imprints of neuronal activity: relationships between the dynamics of cortical blood flow, oxygenation, and volume changes following sensory stimulation. *Proc. Natl. Acad. Sci. U. S. A.* 95, 14826–14831.
- Marchal, G., Rioux, P., Petit-Taboue, M.C., Sette, G., Travers, J.M., Le Puce, C., et al., 1992. Regional cerebral oxygen consumption, blood flow, and blood volume in healthy human aging. *Arch. Neurol.* 49, 1013–1020.
- Matsuo, K., Kato, T., Fukuda, M., Kato, N., 2000. Alteration of hemoglobin oxygenation in the frontal region in elderly depressed patients as measured by near-infrared spectroscopy. *J. Neuropsychiatry Clin. Neurosci.* 12, 465–471.
- Matsuo, K., Kato, N., Kato, T., 2002. Decreased cerebral haemodynamic response to cognitive and physiological tasks in mood disorders as shown by near-infrared spectroscopy. *Psychol. Med.* 32, 1029–1037.
- Meltzer, C.C., Cantwell, M.N., Greer, P.J., Ben-Eliezer, D., Smith, G., Frank, G., et al., 2000. Does cerebral blood flow decline in healthy aging? A PET study with partial-volume correction. *J. Nucl. Med.* 41, 1842–1848.
- Murphy, D.G., DeCarli, C., McIntosh, A.R., Daly, E., Mentis, M.J., Pietrini, P., et al., 1996. Sex differences in human brain morphometry and metabolism: an in vivo quantitative magnetic resonance imaging and positron emission tomography study on the effect of aging. *Arch. Gen. Psychiatry* 53, 585–594.
- Obrig, H., Villringer, A., 2003. Beyond the visible: imaging the human brain with light. *J. Cereb. Blood Flow Metab.* 23, 1–18.
- Oldfield, R.C., 1970. The assessment and analysis of handedness: the Edinburgh inventory. *Neuropsychologia* 9, 97–113.
- Pantano, P., Baron, J.C., Lebrun-Grandie, P., Duquesnoy, N., Bousser, M.G., Comar, D., 1984. Regional cerebral blood flow and oxygen consumption in human aging. *Stroke* 15, 635–641.
- Parks, R.W., Loewenstein, D.A., Dodrill, K.L., Barker, W.W., Yoshii, F., Chang, J.Y., 1988. Cerebral metabolic effects of a verbal fluency test: a PET scan study. *J. Clin. Exp. Neuropsychol.* 10, 565–575.
- Ragland, J.D., Coleman, A.R., Gur, R.C., Glahn, D.C., Gur, R.E., 2000. Sex differences in brain-behavior relationships between verbal episodic memory and resting regional cerebral blood flow. *Neuropsychologia* 38, 451–461.
- Rodriguez, G., Warkentin, S., Risberg, J., Rosadini, G., 1988. Sex differences in regional cerebral blood flow. *J. Cereb. Blood Flow Metab.* 8, 783–789.
- Sakai, K.L., Hashimoto, R., Homae, F., 2001. Sentence processing in the cerebral cortex. *Neurosci. Res.* 39, 1–10.
- Sato, H., Takeuchi, T., Sakai, K.I., 1999. Temporal cortex activation during speech recognition: an optical topography study. *Cognition* 73, B55–B66.
- Schlösser, R., Hutchinson, M., Joseffer, S., Rusinek, H., Saarimaki, A., Stevenson, J., et al., 1998. Functional magnetic resonance imaging of human brain activity in a verbal fluency task. *J. Neurol. Neurosurg. Psychiatry* 64, 492–498.
- Schroeter, M.L., Zysset, S., Kruggel, F., von Cramon, D.Y., 2003. Age dependency of the hemodynamic response as measured by functional near-infrared spectroscopy. *NeuroImage* 19, 555–564.
- Shaywitz, B.A., Shaywitz, S.E., Pugh, K.R., Constable, R.T., Skudlaski, P., Fulbright, R.K., et al., 1995. Sex differences in the functional organization of the brain for language. *Nature* 373, 607–609.
- Silverman, I., Phillips, K., Silverman, L.K., 1996. Homogeneity of effect sizes for sex across spatial tests and cultures: implications for hormonal theories. *Brain Cogn.* 31, 90–94.
- Strangman, G., Boas, D.A., Sutton, J.P., 2002a. Non-invasive neuroimaging using near-infrared light. *Biol. Psychiatry* 52, 679–693.
- Strangman, G., Culver, J.P., Thompson, J.H., Boas, D.A., 2002b. A quantitative comparison of simultaneous BOLD fMRI and NIRS recordings during functional brain activation. *NeuroImage* 17, 719–731.
- Suto, T., Fukuda, M., Ito, M., Uehara, T., Mikuni, M., 2004. Multichannel near-infrared spectroscopy in depression and schizophrenia: cognitive brain activation study. *Biol. Psychiatry* 55, 501–511.
- Toronov, V., Webb, A., Choi, J.H., Wolf, M., Michalos, A., Gratton, E., et al., 2001. Investigation of human brain hemodynamics by simultaneous near-infrared spectroscopy and functional magnetic resonance imaging. *Med. Phys.* 28, 521–527.
- Vikingsstad, E.M., George, K.P., Johnson, A.F., Cao, Y., 2000. Cortical language lateralization in right handed normal subjects using functional magnetic resonance imaging. *J. Neurol. Sci.* 175, 17–27.
- Villringer, A., Planck, J., Hock, C., Schleinkofer, L., Dimagl, U., 1993. Near infrared spectroscopy (NIRS): a new tool to study hemodynamic changes during activation of brain function in human adults. *Neurosci. Lett.* 154, 101–104.
- Watanabe, E., Maki, A., Kawaguchi, F., Takashiro, K., Yamashita, Y., Koizumi, H., et al., 1998. Non-invasive assessment of language dominance with near-infrared spectroscopic mapping. *Neurosci. Lett.* 256, 49–52.
- Yamaguchi, T., Kanno, I., Uemura, K., Shishido, F., Inugami, A., Ogawa, T., et al., 1986. Reduction in regional cerebral metabolic rate of oxygen during human aging. *Stroke* 17, 1220–1228.
- Yamamoto, T., Yamashita, Y., Yoshizawa, H., Maki, A., Iwata, M., Watanabe, E., et al., 1999. Non-invasive measurement of language function by using optical topography SPIE 3597, 230–237.



Research report

Expression profile of mRNAs from rat hippocampus and its application to microarray

Takeshi Tanaka^a, Yukio Horikawa^{b,c,*}, Takanori Kawamoto^a, Noriko Kabe-Sakurai^a, Jun Takeda^{b,c,d}, Masahiko Mikuni^a

^aDepartment of Psychiatry and Human Behavior, Gunma University, Graduate School of Medicine, Gunma, Japan

^bLaboratory of Molecular Genetics, Department of Cell Biology, Institute for Molecular and Cellular Regulation, Gunma University, Gunma, Japan

^cCore Research for Evolutional Science and Technology (CREST), Japan Science and Technology Corporation (JST), Kawaguchi, Japan

^dDivision of Bioregulatory Medicine, Department of Endocrinology, Diabetes and Rheumatology, Gifu University School of Medicine, Gifu, Japan

Accepted 17 June 2004

Available online 23 July 2004

Abstract

Stress refers to physiological or psychological stimuli that disrupt homeostasis and induce pathophysiological conditions due to maladaptive response, sometimes resulting in mental disorders including depression and post-traumatic stress disorder. Severe stress has been shown to induce neuronal atrophy and apoptosis, especially in the hippocampus, which is thought to be a region of the brain important in stress-related disorders. We have analyzed gene expression in rat hippocampus comprehensively to clarify the molecular mechanism of stress-related disorders. In the present study, we identified and catalogued 13,660 partial complementary DNA sequences (expressed sequence tags (ESTs)) of randomly selected clones from a cDNA library of rat hippocampus. Sequence analysis showed that these clones cluster into 7173 non-redundant sequences comprising 1794 clusters and 5379 singletons. As a result of nucleotide and peptide database search, 2594 were found to represent known rat sequences. Of the remaining 4579 genes, 599 non-redundant ESTs represent rat homologs of genes identified in other species or new members of structurally related families. In addition, we illustrate the use of these clone sets by constructing a cDNA microarray focused on genes categorized into 'cell/organism defense'. These ESTs and our own microarray thus provide an improved genomic source for molecular studies of animal models of stress-related disorders.

© 2004 Elsevier B.V. All rights reserved.

Theme: Cellular and molecular biology

Topic: Gene structure and function: general

Keywords: Hippocampus; Stress; Expressed sequence tags (ESTs); cDNA library; Microarray

1. Introduction

The hippocampus is not only crucial in learning and memory but also is especially vulnerable to stress. This region of the brain also is involved in feedback regulation of the hypothalamus–pituitary–adrenal axis, dysfunction of

which is associated with depression [12,30]. The effects of chronic stress on brain function via CRF, ACTH, and glucocorticoids may trigger some of the pathophysiological changes in brain function related to depression and other stress-related disorders. Glucocorticoids are known to influence most brain regions, but have particularly dramatic effects on limbic structures such as hippocampus and amygdala [24]. Recent studies suggest that stress-induced atrophy and loss of hippocampal neurons may contribute to the pathophysiology of depression [6,20]. Interestingly, hippocampal volume is decreased in patients with stress-related disorders, including depression and

* Corresponding author. Laboratory of Molecular Genetics, Department of Cell Biology, Institute for Molecular and Cellular Regulation, Gunma University, 3-39-15 Showa-machi, Maebashi, Gunma 371-8512, Japan. Tel.: +81 27 220 8831; fax: +81 27 220 8889.

E-mail address: yhorikaw@showa.gunma-u.ac.jp (Y. Horikawa).

post-traumatic stress disorder [24,25]. Furthermore, the hippocampus is one of only a few brain regions where the production of neurons occurs throughout the lifetime of animals, including human [7]. Furthermore, hippocampal neurogenesis is influenced by various environmental factors and stimuli [11,21,29]. For example, both acute and chronic stress cause a decrease in cell proliferation [8].

These findings indicate that cell death, neurogenesis, and the more dramatic changes induced by chronic stress occur in hippocampus together with stress-related disorders. To compare gene expression in the hippocampus in normal and an animal model of mental disorder, we analyzed gene expression in this region of the brain by large-scale sequencing of randomly selected clones from the cDNA library to generate expressed sequence tags (ESTs).

We also illustrate one use of these clone sets by constructing a cDNA microarray focused on genes categorized into 'cell/organism defense'. These nonredundant hippocampus clone sets and our own microarray promise to become a useful tool for molecular studies of animal models of stress-related disorders.

2. Materials and methods

2.1. cDNA sequencing

A non-unidirectional cDNA library with inserts larger than ~400 bp, which was constructed using mRNAs from adult rat hippocampus and Lambda ZAP[®] II vector system, was purchased from commercial company (Stratagene, La Jolla, CA, USA). Plasmid DNA were prepared as described previously [28]. Briefly, the non-unidirectional cDNA library was excised *in vivo* from the λ phage into phagemid DNA using the ExAssist[®] helper phage (Stratagene). Phagemid particles were transfected into *Escherichia coli* SOLR (Stratagene) and plated on LB plates containing ampicillin to generate plasmid forms. The colonies were randomly selected from the plates and plasmid DNAs were extracted using the Biomek 2000 miniprep systems (Beckman, Fullerton, CA, USA). The inserts of the cDNA clones were sequenced from both ends. DNA sequencing was performed using an ABI PRISM BigDye Terminator Cycle Sequencing FS Ready Reaction Kit[®] (Applied Biosystems, Foster, CA, USA). The sequencing reaction products were analyzed by an Applied Biosystems DNA sequencer model 377. Quality assessment and base trimming of each sequence were performed using PE Sequencing Analysis 3.3 software (Applied Biosystems). Contaminated vector sequences were removed using Assembly LIGN[®] (copyright by Oxford Molecular Group). Sequences containing less than 1% ambiguous bases longer than 200 bp were counted as good sequences.

2.2. Database analysis of rat hippocampus ESTs

We analyzed ~13,867 ESTs from rat hippocampus with non-redundant nucleotide and peptide sequences extracted *in silico* from GenBank databases at the National Center for Biotechnology Information (NCBI) (<http://www.ncbi.nlm.nih.gov/>). We first removed tracks of ambiguous residues from the obtained ESTs and masked the highly repetitive sequences by RepeatMasker (<http://ftp.genome.washington.edu/RM/RepeatMasker.html>). The resultant sequences were subjected to a BLAST search against a merged database containing daily updates of rat sequences from GenBank. The program BLASTN [2] was used to compare the sequences at the level of the nucleic acids. If a query EST sequence shared more than 95% sequence identity without masked and ambiguous nucleotides and showed a score of more than 365 with any other sequences in the database, it was grouped with the query. If there was at least one sequence in common, groups were merged into a single cluster. An EST sequence that did not belong to any of the clusters is a singleton. To assemble the sequences that belonged in each cluster, we applied the Labo Server[®] system to make contigs (World Fusion, Tokyo, Japan). The EST clones without any match to known genes in the nucleotide database were retrieved by the BLASTX program [2], which was used to conceptually translate the sequence in all six reading frames and compare the sequences with those in the peptide database at NCBI (<http://www.ncbi.nlm.nih.gov/>).

Role categories and subcategories were chosen to encompass a broad view of rat cell biology. Although many categorization schemes might be considered equally valid, we have attempted to group together proteins that share similar functional characteristics or cellular roles rather than by a strict biochemical classification. Roles were assigned according to the known or putative involvement of a gene or protein in a cellular process or pathway as opposed to participation in a specific binding or catalysis function on which Gene Ontology (GO) annotations are based.

We used a seventh broad category, unclassified, for proteins and genes of unknown role or which could not be assigned with confidence based on searches of the literature [1]. The EST clones matching known genes (excluding repetitive elements and probable microbial contaminant sequences) were catalogued into seven general categories (cell division, cell signaling/cell communication, cell structure/motility, cell/organism defense, gene/protein expression, metabolism and unclassified) and subcategorized according to specific function based on the putative functions of the known genes using the Genome Directory (<http://www.tigr.org/tdb/hgi.html>), UniGene, Entrez and PubMed at the NCBI. Two subcategories were included in cell structure/motility, namely, contractile proteins and vesicular transport [1,13].

Table 1
Summary of rat hippocampus ESTs

	Known genes	Unknown genes	Total
Cluster	1282	512	1794
Singleton	1312	4067	5379
Total	2594	4579	7173

2.3. Animals and treatment

Adult Sprague–Dawley rats (Charles River, Yokohama, Japan) were sacrificed by decapitation, and hippocampus were quickly dissected on an ice plate, immediately frozen with liquid nitrogen and stored at -80°C until RNA isolation. All procedures were performed in accordance with our institutional guidelines after obtaining the permission of the Laboratory Animal Committee of Gunma University.

2.4. Construction of an original cDNA microarray

For future investigation of the genotype of stress responses in the nerve system, 115 clones related in 'cell/organism defense' were selected from the collected ESTs. Clones were amplified by PCR using ExTaq[®] (TaKaRa Shuzou, Kyoto, Japan) in a 50 μl reaction mixture and PCR was performed 12 times for each clone. Amplification was performed as follows: 3 min at 94°C for initial denaturation, 35 cycles of 94°C denaturing for 30 s, 60°C annealing for 30 s and 72°C extension for 1 min, followed by a final extension at 72°C for 10 min. The quality and quantity of purified PCR product was confirmed using 1.2% agarose gel electrophoresis. One hundred and four of 115 clones that gave a single band then were used to construct an original cDNA microarray. Purified PCR products of each clone were resuspended in $3\times\text{SSC}$ so that concentrations of nucleotide would be about 1 $\mu\text{g}/\mu\text{l}$. cDNA solutions were spotted onto poly-L-lysine-coated microarray slides (Matsunami Glass, Japan) using a capillary pen styled arrayer (OmniGrid[™]). cDNA spotted slides were then exposed to 120 mJ of 254 nm light to crosslink DNA on slides. Lambda phage DNA were spotted as negative controls, and GAPDH and 18S rRNA were used as positive controls.

Table 2
Redundancy of nucleotide sequences from the cDNA clones

Redundancy	No. of groups	Percentage
1	5379	75.0
2	953	13.3
3	348	4.9
4	165	2.3
5	85	1.2
6–10	158	2.2
11–20	62	0.9
21–50	22	0.3
51–100	0	0.0
>100	2	0.0

2.5. Hybridization and analysis

Total RNA was extracted from hippocampus using Qiagen RNeasy RNA extraction Kit (Qiagen, Valencia, CA, USA). We confirmed extraction of a high yield of intact total RNA by 1.2% formaldehyde agarose gel. The cDNA probes were generated by RNA reverse transcription under BD PowerScript Reverse Transcriptase (Clontech, Palo Alto, CA, USA) with a modified oligo (dT) primer (the BD SMART CDS Primer IIA, Clontech). cDNA probes then were labeled with a modified indirect labeling protocol using BD Atlas SMART Fluorescent Probe Amplification Kit[®] (Clontech). Briefly, primary aliphatic amino groups are incorporated through primer extension using a dNTP mix, which includes the dTTP analog, aminoallyl-dUTP. The aminoallyl-dUTP-labeled cDNA probes then are labeled with Cy3 dye (Amersham Biosciences, Piscataway, NJ, USA). In preparation for hybridization, the cDNA pellets were resuspended in 25 μl sterile deionized water. The probes then were mixed with 20 μg poly dA, 20 μg tRNA and 20 μg mouse Cot1 DNA, and finally resuspended in 50 μl of $3.4\times\text{SSC}/0.5\%$ SDS. The probe was incubated at 95°C for 5 min, transferred to a prehybridized glass array and incubated for 18 h in a hybridization chamber (KakenGeneqs, Chiba, Japan) at 65°C . After the hybridization, glass arrays were washed three times with agitation in the following solutions: $2\times\text{SSC}/0.1\%$ SDS for 2 min, $1\times\text{SSC}/0.1\%$ SDS for 2 min and $0.2\times\text{SSC}/0.1\%$ SDS for 2 min at room temperature. Arrays then were dried by centrifugation in a slide rack for 2 min at 800 rpm. All slides were scanned immediately using a ScanArray[®] Lite (PerkinElmer, Boston, MA, USA). Image analysis was performed with QuantArray (PerkinElmer) and background intensities were determined by the median pixel values.

3. Results

3.1. Characterization of rat hippocampus ESTs

A total of ~15,000 random clones from a non-unidirectional cDNA library were partially sequenced from the 3' - and 5' -end to generate 13,660 sequences with good quality. Such large-scale sequencing generally provides highly redundant ESTs that can be aligned and assembled for a set of unique genes. After 985 repetitive (7.1%) sequences and 323 mitochondrial (2.3%) DNAs were removed, the remaining ESTs were assembled into non-redundant sequence groups. The clustering analysis generated 7173 non-redundant sequences comprising 1794 groups of sequences and 5379 singletons (Table 1). Of these, 2594 were known genes. Relative frequencies of the ESTs for each gene reflect the average level of expression of the corresponding mRNAs in the pooled tissues. Since groups with redundancy of 1–5 times accounted for 96.6% of the groups, our massive sequencing was clearly effective in

Table 3
List of highly redundant cDNA clones

Redundancy	Gene products	Cellular function
119	myelin basic protein	cell structure/motility
111	proteolipid protein	cell structure/motility
50	synaptic vesicle glycoprotein 2 b	vesicular transport
47	hydroxy- δ -5-steroid dehydrogenase, 3 β - and steroid δ -isomerase 1	lipid
44	myelin-associated oligodendrocytic basic protein	cell structure/motility
42	polyubiquitin	posttranslation modification/targeting
39	SNAP25 interacting protein	vesicular transport
38	calmodulin 1	effectors/modulators
35	glial fibrillary acidic protein	cytoskeletal
35	heat shock protein 8	stress response
34	eukaryotic translation elongation factor 1 α 1	translation factors
33	β -spectrin 3	cytoskeletal
32	calcium/calmodulin-dependent protein kinase II α subunit	protein modification
32	SPARC-like 1	extracellular matrix
28	kinesin family member 5C	microtubule-associated proteins/motors
27	amyloidogenic glycoprotein (rAG), cognate of human A4 amyloid precursor protein	cell adhesion
26	development-related protein	unclassified
26	glutamine synthetase 1	amino acid
24	ATPase, Na ⁺ K ⁺ transporting, α 2	transport
24	heat shock protein 1, α	stress response
23	microtubule-associated protein 2	microtubule-associated proteins/motors
22	ATPase Na ⁺ /K ⁺ transporting β 1 polypeptide	transport
21	heat shock protein 90	stress response
21	stearoyl-coenzyme A desaturase 2	lipid
19	calmodulin 3	effectors/modulators
19	ribonucleotide reductase M2 subunit	nucleotide
18	myelin and lymphocyte protein	unclassified
18	neurochondrin	unclassified
18	reticulon 3	unclassified
18	syntaxin binding protein 1	vesicular transport
17	α -spectrin 2	cytoskeletal
17	cadherin 22	cell adhesion
17	glutamate oxaloacetate transaminase 1	amino acid
17	<i>Rattus norvegicus</i> clone RP31-464J4 strain Brown Norway	unclassified
17	tyrosine 3-monooxygenase/tryptophan 5-monooxygenase activation protein, ζ polypeptide	protein modification
16	aldolase C, fructose-biphosphate	sugar/glycolysis
16	α -tubulin	cytoskeletal
16	glutamate receptor, ionotropic, 2	receptors
16	prion protein	transcription factors

Table 3 (continued)

Redundancy	Gene products	Cellular function
16	protein carrying the RING-H2 sequence motif	posttranslation modification/targeting
16	protein tyrosine phosphatase, receptor type, D	receptors
15	adaptor-related protein complex 2, μ 1 subunit	vesicular transport
15	carboxypeptidase E	protein turnover
15	dynamin 1	cytoskeletal
15	neural visinin-like Ca ²⁺ -binding protein type 2	effectors/modulators
15	neuronal pentraxin receptor	receptors
15	solute carrier family 1, member 3	channels/transport
14	ATPase, H ⁺ transporting, lysosomal (vacuolar proton pump), β 56/58 kDa, isoform 2	transport
14	chimerin (chimaerin) 1	intracellular transducers
14	DEAD (Asp-Glu-Ala-Asp) box polypeptide 5	RNA processing
14	myelin-associated glycoprotein	cell structure/motility
14	<i>N</i> -ethylmaleimide sensitive factor	carrier proteins/membrane transport
14	prosaposin	unclassified
14	triosephosphate isomerase 1	sugar/glycolysis
13	growth arrest specific 7	cell cycle
13	protein tyrosine kinase 2 β	protein modification
13	SNRPN upstream reading frame	unclassified
13	system N1 Na ⁺ and H ⁺ -coupled glutamine transporter	channels/transport
13	tumor differentially expressed 1	unclassified
12	ankyrin 3 (G)	cytoskeletal
12	brain Ntab mRNA sequence	unclassified
12	C1-13 gene product	unclassified
12	eukaryotic translation elongation factor 2	translation factors
12	hippocalcin	effectors/modulators
12	nasal embryonic LHRH factor	unclassified
12	<i>Rattus norvegicus</i> clone RP31-422M21 strain Brown Norway	unclassified
12	S100 protein, β polypeptide	effectors/modulators
12	similar to RIKEN cDNA 1700001E04	unclassified
12	synaptotagmin 1	effectors/modulators
12	tyrosine 3-monooxygenase/tryptophan 5-monooxygenase activation protein, γ polypeptide	protein modification
12	v-raf-1 murine leukemia viral oncogene homolog 1	cell division
11	adaptor-related protein complex 3, β 2 subunit	vesicular transport
11	amyloid β (A4) precursor-like protein 1	protein turnover
11	ATPase, Na ⁺ K ⁺ transporting, α 3 subunit	transport
11	C1q-like	unclassified
11	cytoplasmic FMR1 interacting protein 2	unclassified
11	diacylglycerol kinase ζ	lipid
11	glycoprotein m6b	cell structure/motility

(continued on next page)

Table 3 (continued)

Redundancy	Gene products	Cellular function
11	inositol 1,4,5-triphosphate receptor 1	receptors
11	mitogen-activated protein kinase 8 interacting protein 3	protein modification
11	nel-like 2 homolog (chicken)	unclassified
11	neurexin 1	cell adhesion
11	nucleolar protein 3 (apoptosis repressor with CARD domain)	unclassified
11	similar to expressed sequence C85658	unclassified
11	thymus cell antigen 1, θ	immunology
11	tyrosine 3-monooxygenase/tryptophan 5-monooxygenase activation protein, θ polypeptide	protein modification
10	adenomatous polyposis coli	cell division
10	synaptosomal-associated protein	cell division
10	ATP/GTP binding protein 1	intracellular transducers
10	cyclic nucleotide phosphodiesterase 1	metabolism
10	nucabin 2	cytoskeletal
10	neurofilament 3, medium	cytoskeletal
10	dystonin	extracellular matrix
10	limbic system-associated membrane protein	immunology
10	bruno-like 4, RNA binding protein (<i>Drosophila</i>)	RNA processing
10	tripartite motif protein 3	transcription factors
10	similar to ORF2 consensus sequence encoding endonuclease and reverse transcriptase minus RNaseH	transcription factors
10	protein phosphatase 2a, catalytic subunit, α isoform	protein modification
10	phosphofructokinase, platelet	sugar/glycolysis
10	Nogo-A	unclassified
10	sperm membrane protein (YWK-II)	unclassified

identifying a larger number of non-redundant mRNAs expressed at moderate levels (Table 2). Approximately 2.2% of the ESTs were identified 6–10 times. One hundred and one abundant sequences identified more than nine times (1.4%) are shown in Table 3. Of these, myelin basic protein (118 times) and brain myelin proteolipid protein (PLP) (111 times), the major extrinsic myelin protein and the major integral myelin membrane protein, respectively, are most abundant in this library.

3.2. Expression profile of known genes in rat hippocampus

The ESTs showing identity or high similarity to known genes were classified into seven major categories on the basis of putative general functions of the protein encoded, as described previously (categories; ‘cell division’, ‘cell signaling/communication’, ‘cell structure/motility’, ‘cell/organism defense’, ‘gene/protein expression’, ‘metabolism’ and

‘unclassified’) [1,13]. In total, 2594 known genes are represented in the classified data set (supplement at <http://imcr.showa.gunma-u.ac.jp/lab/genetics/RHippocampus.zip>). In concordance with the results in ESTs from brain observed by Adams et al., the largest category of genes was ‘cell signaling and communication’ except for the category ‘unclassified’ (618 genes, 23.8%) (Fig. 1). Successively smaller categories were ‘gene/protein expression’ (19.1%), ‘metabolism’ (13.8%), ‘cell structure/motility’ (9.5%), ‘cell division’ (4.8%) and ‘cell/organism defense’ (4.4%). ESTs lacking sufficient information to be classified constituted the remainder (24.5%). To further analyze the molecular complexity, each major category was subdivided according to the putative specific functions of the proteins (supplement at <http://imcr.showa.gunma-u.ac.jp/lab/genetics/RHippocampus.zip>). For example, the largest category, ‘cell signaling and communication’, was subdivided into eight subgroups (Fig. 2). Of these, ‘protein modification’ includes the largest number of non-redundant genes (145 genes) and ESTs for that function are also identified most frequently (429 ESTs for 145 different proteins).

3.3. Rat homologs of known genes and new members of gene families

In this study, 63.8% of the non-redundant ESTs did not match any of the known genes in the nucleotide database. To identify novel rat genes encoding proteins structurally related to the known proteins, we performed BLASTX search in the peptide databases using 4579 ESTs, with P -value of 10^{-10} and score of 60 as the cut off for significant similarity. Five hundred and ninety-nine non-redundant ESTs match this condition and, of these, 169 ESTs represent rat homologs of genes identified in mouse or new members of structurally related families in rat (Table 4). Of these, the proteins similar to NEDD-4 protein, retrovirus-related POL polyproteins and zinc finger proteins were most abundant. Functional analyses of the proteins identified through this approach should clarify the role of new members of structurally related families in hippocampus. The remaining ESTs (3980 genes) were not related to any other sequences in the databases. As found in similar large-scale cDNA sequencing studies carried out in other tissues, about 50% of the clones appear to be derived from genes that have not previously been described.

3.4. Construction of an original cDNA microarray

In this study, we illustrate one use of these clone sets by constructing a cDNA microarray focused on genes categorized into ‘cell/organism defense’ for use in further molecular studies of animal models of stress-related disorders. The hybridization pattern of normal adult rat hippocampal cDNA by our own microarray is shown in Fig. 3A and B. The 104 clones, 2 positive and 1 negative controls are spotted on the glass 10 times each. (Table 5). A

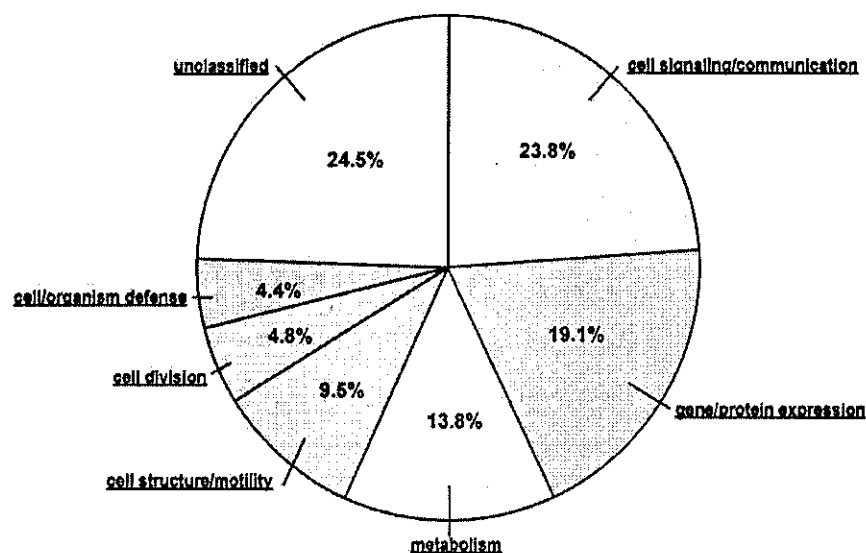


Fig. 1. Functional distribution of known genes in rat hippocampus. ESTs showing identity or high similarity to known genes were classified into seven major categories on the basis of the putative general functions of the protein encoded.

number of heat shock proteins (HSPs) and stress inducible proteins are certainly expressed also in normal rat hippocampus. As shown in Fig. 3 C, there was significant correlation between the frequencies of observed ESTs and the signal intensities of the spots ($r=0.713$).

4. Discussion

Expression profiling using serial analysis of gene expression (SAGE) tags and ESTs is a potent method for identifying and characterizing both known and novel genes in a given tissue. Over the past few years, cDNA libraries

have been prepared from many tissues and cell lines, from which a large number of SAGE tags and ESTs have been studied. An expression profile of 30,000 genes in rat hippocampus using the SAGE method has been reported previously [5]. While SAGE analysis is unique in its ability to quantify gene expression in a given tissue with extremely high throughput, there are several limitations for the analysis of the data. For example, SAGE generates tags from the most 3' *-Nla*III restriction site, but only on those mRNAs that have the site. Therefore, SAGE may under-perform because specific transcripts may be missed due to the absence of a recognition site for the anchoring enzyme or GC-content bias [17]. In addition, tag to gene

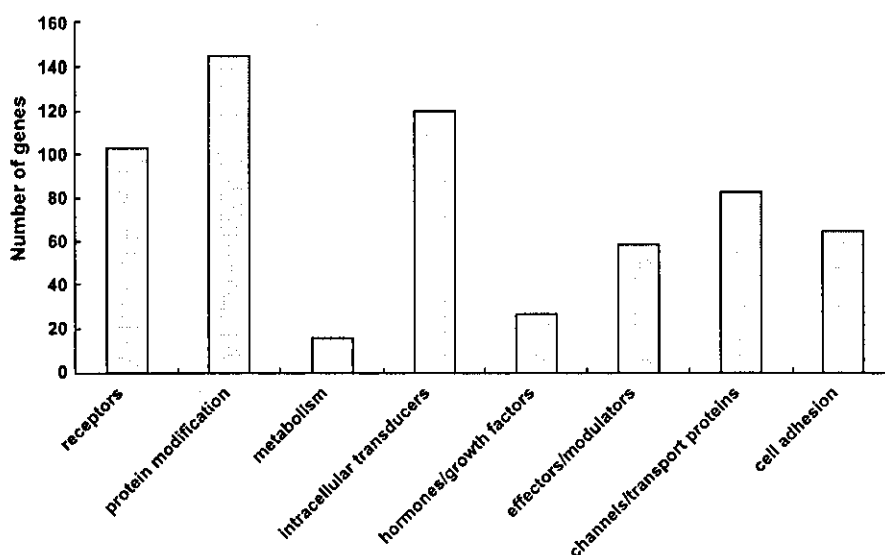


Fig. 2. Subclasses of the cell signaling/communication category. The largest category in Fig. 1 was subdivided into eight subgroups. Of these, the protein modification subgroup contains the largest number of non-redundant genes.

Table 4
Homologs of known genes and new members of gene families

Gene name	Species	Score	P-value	No.
14-3-3 protein eta	<i>Mus musculus</i>	85	4.00E-17	1
60S ribosomal protein L10	<i>Mus musculus</i>	58	1.00E-08	1
60S ribosomal protein L14	<i>Rattus norvegicus</i>	88	7.00E-26	1
60S ribosomal protein L34	<i>Mus musculus</i>	106	3.00E-23	1
Acetyl-CoA acetyltransferase, mitochondrial precursor	<i>Rattus norvegicus</i>	73	3.00E-13	1
Acyl-coenzyme A oxidase 1, peroxisomal	<i>Rattus norvegicus</i>	104	4.00E-23	1
AF-10 protein	<i>Mus musculus</i>	125	4.00E-29	1
Alcohol dehydrogenase class III	<i>Rattus norvegicus</i>	219	2.00E-60	1
α -Actinin 3	<i>Mus musculus</i>	199	3.00E-51	1
Amine oxidase	<i>Rattus norvegicus</i>	78	3.00E-15	1
Amyloid-like protein 1 precursor	<i>Mus musculus</i>	150	5.00E-37	1
Armadillo repeat protein deleted in velo-cardio-facial syndrome homolog	<i>Mus musculus</i>	116	3.00E-26	1
Armadillo repeat protein deleted in velo-cardio-facial syndrome homolog	<i>Mus musculus</i>	114	1.00E-25	1
Armadillo repeat protein deleted in velo-cardio-facial syndrome homolog	<i>Mus musculus</i>	51	7.00E-07	1
ATP synthase A chain	<i>Mus musculus</i>	56	1.00E-08	1
ATP-dependent DNA helicase II, 70-kDa subunit	<i>Mus musculus</i>	70	2.00E-12	1
Basement membrane-specific heparan sulfate proteoglycan core protein precursor	<i>Mus musculus</i>	87	1.00E-17	1
BCL2/adenovirus E1B 19-kDa protein-interacting protein 2	<i>Mus musculus</i>	134	6.00E-32	1
β -Chimerin	<i>Rattus norvegicus</i>	109	3.00E-24	1
β -Secretase precursor	<i>Rattus norvegicus</i>	99	6.00E-21	1
BRCA1-associated RING domain protein 1	<i>Rattus norvegicus</i>	77	2.00E-14	1
C-Rel proto-oncogene protein	<i>Mus musculus</i>	138	9.00E-38	1
Calcium-binding mitochondrial carrier protein Aralar2	<i>Mus musculus</i>	67	9.00E-12	1
cAMP-dependent protein kinase type I- β regulatory chain	<i>Rattus norvegicus</i>	130	2.00E-30	3

Table 4 (continued)

Gene name	Species	Score	P-value	No.
cAMP-dependent protein kinase type II- α regulatory chain	<i>Rattus norvegicus</i>	58	3.00E-17	2
Carbonic anhydrase XIV precursor	<i>Mus musculus</i>	57	2.00E-08	1
Carboxypeptidase H precursor	<i>Rattus norvegicus</i>	173	2.00E-43	1
Cathepsin B precursor	<i>Rattus norvegicus</i>	97	6.00E-21	1
Chloride channel protein 6	<i>Mus musculus</i>	260	9.00E-70	1
Chromobox protein homolog 6	<i>Mus musculus</i>	192	4.00E-50	1
Cofilin, muscle isoform	<i>Mus musculus</i>	52	2.00E-07	2
Cyclic-AMP-dependent transcription factor ATF-5	<i>Mus musculus</i>	69	5.00E-12	1
Cytochrome <i>B</i>	<i>Rattus norvegicus</i>	70	2.00E-12	1
Cytochrome <i>c</i> oxidase polypeptide II	<i>Mus musculus</i>	104	7.00E-23	1
Cytohesin 2	<i>Mus musculus</i>	64	2.00E-10	1
Density-regulated protein	<i>Mus musculus</i>	115	6.00E-26	1
Destrin	<i>Mus musculus</i>	145	2.00E-35	1
Developmentally regulated GTP-binding protein 1	<i>Mus musculus</i>	150	9.00E-37	1
DGCR6 protein	<i>Mus musculus</i>	84	6.00E-17	1
Disks large-associated protein 1	<i>Rattus norvegicus</i>	103	6.00E-23	1
DNA binding protein URE-B1	<i>Rattus norvegicus</i>	79	5.00E-15	1
DNA-binding protein SATB1	<i>Mus musculus</i>	62	4.00E-10	1
DnaJ homolog subfamily C member 4	<i>Mus musculus</i>	85	2.00E-17	1
Dual specificity protein phosphatase 8	<i>Mus musculus</i>	161	5.00E-40	1
Ectoderm-neural cortex-1 protein	<i>Mus musculus</i>	68	5.00E-16	1
Ectoderm-neural cortex-1 protein	<i>Mus musculus</i>	83	2.00E-16	1
Ectonucleotide pyrophosphatase/phosphodiesterase 1	<i>Mus musculus</i>	55	8.00E-08	2
Elongation factor 2	<i>Rattus norvegicus</i>	99	5.00E-21	1
Enhancer of zeste homolog 1	<i>Mus musculus</i>	62	6.00E-10	1
Exostosin-1	<i>Mus musculus</i>	104	6.00E-23	1
FK506-binding protein precursor	<i>Mus musculus</i>	67	2.00E-11	1
Focal adhesion kinase 1	<i>Rattus norvegicus</i>	102	1.00E-22	1
Galactocerebrosidase precursor	<i>Mus musculus</i>	90	7.00E-19	1

Table 4 (continued)

Gene name	Species	Score	P-value	No.
Glucose-6-phosphate isomerase	<i>Mus musculus</i>	159	3.00E-39	1
Glutamate receptor 1 precursor	<i>Mus musculus</i>	116	3.00E-26	2
Glutamate receptor, ionotropic kainate 5 precursor	<i>Rattus norvegicus</i>	56	2.00E-08	1
Guanine nucleotide exchange factor DBS	<i>Rattus norvegicus</i>	89	5.00E-18	1
Guanine nucleotide releasing protein (GNRP) (P140 Ras-GRF)	<i>Rattus norvegicus</i>	100	7.00E-22	1
Guanine nucleotide-binding protein β subunit 5	<i>Mus musculus</i>	79	2.00E-15	3
Guanine nucleotide-binding protein G(q), α subunit	<i>Rattus norvegicus</i>	59	2.00E-09	2
Guanine nucleotide-binding protein G(S), α subunit	<i>Mus musculus</i>	99	1.00E-21	1
Histidine-rich membrane protein Kc4	<i>Mus musculus</i>	85	4.00E-17	1
Histone deacetylase 6	<i>Mus musculus</i>	188	4.00E-48	2
Importin α -3 subunit	<i>Mus musculus</i>	78	5.00E-15	1
Inhibitor of nuclear factor κ -B kinase α subunit	<i>Mus musculus</i>	85	9.00E-28	1
Integral membrane protein 2B	<i>Mus musculus</i>	74	1.00E-13	1
Integrin α -6 precursor	<i>Mus musculus</i>	72	9.00E-13	2
Inter- α -trypsin inhibitor heavy chain H3 precursor	<i>Rattus norvegicus</i>	102	4.00E-22	1
Interferon- α/β receptor α chain precursor	<i>Mus musculus</i>	65	3.00E-11	1
Kinesin-like protein KIF3A	<i>Mus musculus</i>	74	1.00E-13	1
Lamin B3	<i>Mus musculus</i>	125	7.00E-29	1
Latent transforming growth factor β binding protein 1 precursor	<i>Rattus norvegicus</i>	95	9.00E-20	1
Leukocyte tyrosine kinase receptor precursor	<i>Mus musculus</i>	78	9.00E-15	1
LIM/homeobox protein Lhx6.1	<i>Mus musculus</i>	80	1.00E-15	1
Low molecular weight phosphotyrosine protein phosphatase ACP1/ACP2	<i>Rattus norvegicus</i>	97	2.00E-20	1
Lysosomal α -mannosidase precursor	<i>Mus musculus</i>	136	2.00E-32	1
Lysosomal α -mannosidase precursor	<i>Mus musculus</i>	110	1.00E-32	1

Table 4 (continued)

Gene name	Species	Score	P-value	No.
Methionyl-tRNA formyltransferase, mitochondrial precursor	<i>Mus musculus</i>	87	2.00E-17	1
Methylmalonate-semialdehyde dehydrogenase [acylating], mitochondrial precursor	<i>Rattus norvegicus</i>	84	1.00E-16	1
Microtubule-associated protein 1A	<i>Mus musculus</i>	73	1.00E-13	1
Microtubule-associated protein 4	<i>Mus musculus</i>	95	6.00E-20	2
Mitochondrial trifunctional enzyme α subunit precursor	<i>Rattus norvegicus</i>	112	3.00E-25	1
Mitogen-activated protein kinase 7	<i>Mus musculus</i>	125	4.00E-29	1
Myelin and lymphocyte protein	<i>Rattus norvegicus</i>	58	1.00E-08	1
Myelin basic protein S	<i>Rattus norvegicus</i>	90	2.00E-18	1
Myotubularin-related protein 3	<i>Mus musculus</i>	50	4.00E-07	1
NADPH/adrenodoxin oxidoreductase, mitochondrial precursor	<i>Rattus norvegicus</i>	72	5.00E-13	1
NEDD-4 protein	<i>Mus musculus</i>	56	3.00E-08	1
NEDD-4 protein	<i>Mus musculus</i>	54	1.00E-07	1
NEDD-4 protein	<i>Mus musculus</i>	54	1.00E-07	1
NEDD-4 protein	<i>Mus musculus</i>	54	1.00E-07	1
NEDD-4 protein	<i>Mus musculus</i>	53	4.00E-07	1
NEDD-4 protein	<i>Mus musculus</i>	53	2.00E-07	1
NEDD-4 protein	<i>Mus musculus</i>	51	8.00E-07	1
NEDD-4 protein	<i>Mus musculus</i>	56	4.00E-08	1
NEDD-4 protein	<i>Mus musculus</i>	54	5.00E-08	1
NEDD-4 protein	<i>Mus musculus</i>	53	1.00E-07	1
Neighbor of A-kinase anchoring protein 95	<i>Mus musculus</i>	88	1.00E-17	1
Neural Wiskott-Aldrich syndrome protein	<i>Rattus norvegicus</i>	125	1.00E-29	1
Neuroendocrine convertase 3 precursor	<i>Mus musculus</i>	70	3.00E-12	2
Neuronal membrane glycoprotein M6-A	<i>Mus musculus</i>	56	1.00E-08	2
Neuronal-specific septin 3	<i>Mus musculus</i>	55	1.00E-07	3
NGFI-A binding protein 1	<i>Rattus norvegicus</i>	92	7.00E-19	1
Nidogen-2 precursor	<i>Mus musculus</i>	50	2.00E-12	2
NK-tumor recognition protein	<i>Mus musculus</i>	120	2.00E-27	1
Nucleolin	<i>Rattus norvegicus</i>	57	8.00E-09	2
Numb-like protein	<i>Mus musculus</i>	213	2.00E-55	1
Peroxisomal targeting signal 2 receptor	<i>Mus musculus</i>	59	7.00E-09	1

(continued on next page)

Table 4 (continued)

Gene name	Species	Score	P-value	No.
Phosphatidylinositol-glycan-specific phospholipase D1 precursor	<i>Mus musculus</i>	127	1.00E-29	1
Phospholipase D2	<i>Rattus norvegicus</i>	58	1.00E-08	1
Phospholipid hydroperoxide glutathione peroxidase, mitochondrial precursor	<i>Rattus norvegicus</i>	114	6.00E-26	1
Polyadenylate-binding protein 1	<i>Mus musculus</i>	61	3.00E-10	1
Potential phospholipid-transporting ATPase IIA	<i>Mus musculus</i>	54	4.00E-08	1
Pristanoyl-CoA oxidase	<i>Rattus norvegicus</i>	82	2.00E-16	1
Probable calcium-binding protein Dd112	<i>Mus musculus</i>	58	1.00E-08	1
Probable cation-transporting ATPase 1	<i>Mus musculus</i>	130	4.00E-31	1
Prostaglandin F2- α receptor regulatory protein precursor	<i>Rattus norvegicus</i>	74	2.00E-13	1
Protein kinase C, γ type	<i>Mus musculus</i>	129	5.00E-30	1
Proto-oncogene tyrosine-protein kinase MER precursor	<i>Rattus norvegicus</i>	68	1.00E-11	1
Protocadherin 3 precursor	<i>Rattus norvegicus</i>	120	9.00E-28	1
Putative protein C21orf62 homolog	<i>Mus musculus</i>	185	6.00E-47	3
Ras-related protein Rab-1B	<i>Rattus norvegicus</i>	113	1.00E-25	1
Regulator of G-protein signaling 5	<i>Rattus norvegicus</i>	97	9.00E-21	1
Retrovirus-related POL polyprotein	<i>Mus musculus</i>	146	1.00E-35	1
Retrovirus-related POL polyprotein	<i>Mus musculus</i>	52	4.00E-07	1
Retrovirus-related POL polyprotein	<i>Mus musculus</i>	134	1.00E-31	1
Retrovirus-related POL polyprotein	<i>Mus musculus</i>	94	2.00E-19	1
Retrovirus-related POL polyprotein	<i>Mus musculus</i>	75	3.00E-14	1
Retrovirus-related POL polyprotein	<i>Mus musculus</i>	65	7.00E-11	1
Retrovirus-related POL polyprotein	<i>Mus musculus</i>	60	2.00E-09	1
Retrovirus-related POL polyprotein	<i>Mus musculus</i>	59	3.00E-15	2
Retrovirus-related POL polyprotein	<i>Mus musculus</i>	56	5.00E-08	1
RING finger protein 27	<i>Mus musculus</i>	147	9.00E-36	2
RING finger protein 4	<i>Rattus norvegicus</i>	65	3.00E-11	1

Table 4 (continued)

Gene name	Species	Score	P-value	No.
Semaphorin 4D precursor	<i>Mus musculus</i>	91	2.00E-18	1
Semaphorin 5A precursor	<i>Mus musculus</i>	121	2.00E-28	1
Semaphorin 6B precursor	<i>Rattus norvegicus</i>	61	2.00E-09	1
Septin 2	<i>Mus musculus</i>	87	3.00E-17	1
Serine/threonine protein kinase 25	<i>Mus musculus</i>	70	9.00E-13	7
Serine/threonine-protein kinase 19	<i>Mus musculus</i>	114	9.00E-26	1
Single-minded homolog 2	<i>Mus musculus</i>	68	9.00E-12	1
Sodium/calcium exchanger 2 precursor	<i>Rattus norvegicus</i>	73	1.00E-13	1
SOX-13 protein	<i>Mus musculus</i>	149	2.00E-36	1
Splicing factor 3B subunit 1	<i>Mus musculus</i>	123	7.00E-29	1
SSXT protein	<i>Mus musculus</i>	71	7.00E-13	1
Surfeit locus protein 6	<i>Mus musculus</i>	58	2.00E-10	1
Synaptotagmin 2	<i>Rattus norvegicus</i>	70	4.00E-12	1
T-cell receptor α chain V region 2B4 precursor	<i>Mus musculus</i>	80	3.00E-15	3
T-complex protein 1, δ subunit	<i>Mus musculus</i>	53	2.00E-07	1
TLM protein	<i>Mus musculus</i>	62	8.00E-10	5
Transcription factor 17	<i>Mus musculus</i>	86	7.00E-17	1
Ubiquinol-cytochrome C reductase complex core protein I, mitochondrial precursor	<i>Mus musculus</i>	205	5.00E-53	1
Ubiquitin carboxyl-terminal hydrolase 2	<i>Mus musculus</i>	127	3.00E-30	2
Uridine kinase	<i>Mus musculus</i>	127	7.00E-30	1
Voltage-gated potassium channel protein Kv3.1	<i>Mus musculus</i>	109	1.00E-24	1
VPS26 protein homolog	<i>Mus musculus</i>	134	1.00E-31	1
VPS26 protein homolog	<i>Mus musculus</i>	74	5.00E-14	1
Werner syndrome helicase homolog	<i>Mus musculus</i>	159	3.00E-39	1
X inactive specific transcript protein	<i>Mus musculus</i>	49	5.00E-07	1
Zinc finger homeobox protein 1b	<i>Mus musculus</i>	137	3.00E-33	1
Zinc finger protein 27	<i>Mus musculus</i>	57	1.00E-08	1
Zinc finger protein 37	<i>Mus musculus</i>	86	3.00E-17	1
Zinc finger protein 37	<i>Mus musculus</i>	77	1.00E-14	1
Zinc finger protein 46	<i>Mus musculus</i>	135	2.00E-32	1
Zinc finger protein 60	<i>Mus musculus</i>	136	2.00E-32	1
Zinc finger protein 90	<i>Mus musculus</i>	94	2.00E-19	1
Zinc finger protein 92	<i>Mus musculus</i>	219	3.00E-59	1
Zinc-finger protein RFP	<i>Mus musculus</i>	84	1.00E-16	1

mapping is not completely definitive, as some tags correspond to several genes. Furthermore, incorrect tag counts can arise from incomplete digestion or alternative

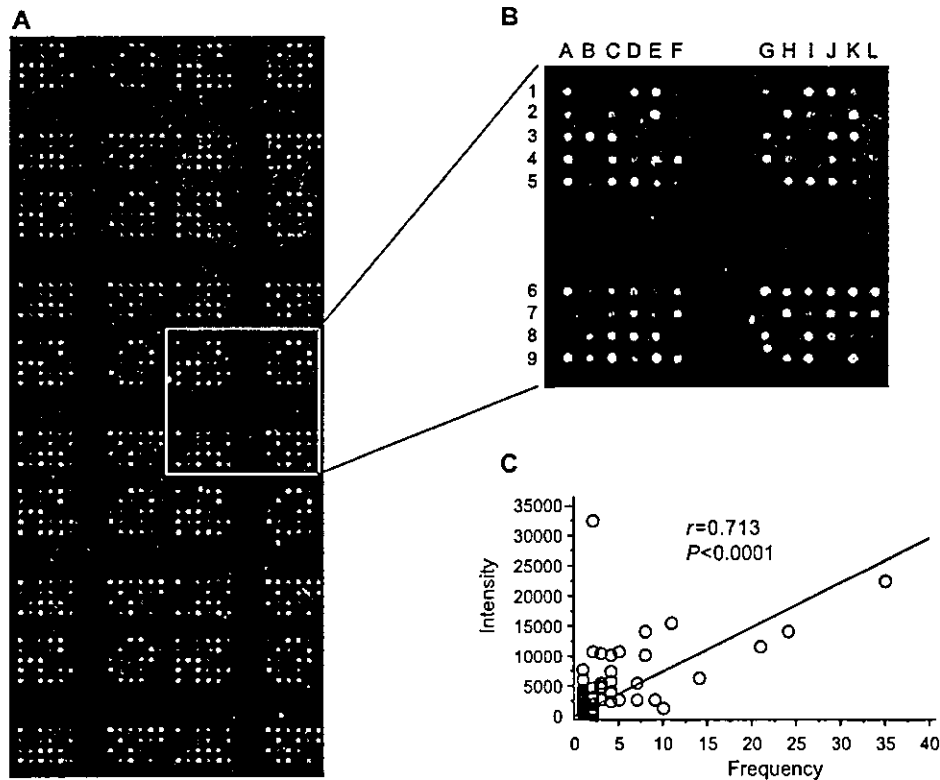


Fig. 3. (A) Hybridization pattern of normal adult rat hippocampal cDNA. The 104 EST clones, 2 positive and 1 negative controls are spotted on the glass 10 times each. (B) Zoom up figure of one sub-array. There are 107 spots in each sub-array. (C) The correlation between the frequencies of observed ESTs and the signal intensities of the spots. There is significant correlation between the frequencies and the signal intensities of the ESTs ($r=0.713$).

polyadenylation, giving rise to multiple tags derived from a single transcript.

However, there has been no report of large-scale generation of ESTs from rat hippocampus. EST analysis has certain advantages over other methods such as SAGE for examining the transcript repertoire of tissues. In particular, EST sequences that cover regions of the coding sequence can reveal variant transcripts and splice forms, many of which have functional significance.

In this study, we describe a collection of 13,660 hippocampus-related ESTs representing 7173 different transcripts. With respect to overall EST distribution (i.e. known gene matches), the results in rat hippocampus in this study differ somewhat from those obtained from other tissues. The largest category of function has been reported to be gene/protein expression in studies of ESTs in tissues other than brain [1,13,15]. The largest number of genes obtained from the rat hippocampus cDNA library encoded proteins related to 'cell signaling and communication', as in earlier EST study of brain [1]. The functional categorization of known genes reflects general differences in gene expression between different tissues, and may reflect tissue-specific function. For example, calmodulin and CAMK II, genes involved in 'protein modification' or 'cell signaling/communication' were identified most frequently in this research, and play an important role in the early stages of

LTP (Long-term potentiation) in hippocampus [9,19,26]. Genes of mitogen-activated protein kinase signaling that belong to the core signaling pathways involved in memory storage [16,18,27] also were found frequently. Tyrosine 3-monooxygenase/tryptophan 5-monooxygenase activation proteins were found in this library abundantly, and play a role in the regulation of serotonin and biosynthesis of brain noradrenaline, reuptake of which is inhibited by antidepressant drugs [14]. In this study, there was also a larger portion of unclassified genes in hippocampus (24.5%) due, at least in part, to the large numbers of hypothetical proteins generated by recent high throughput genome sequencing efforts.

Although the rat genome project has been released [10], a significant fraction of the genes are hypothetical, revealed only by a computer prediction program. Thus, hippocampal transcripts provide a richer resource for analysis of novel genes related to known proteins. This catalog of expressed genes should facilitate the development of tissue-specific cDNA microarray technology.

Various kinds of stress induce the synthesis of stress proteins that protect cells from subsequent lethal stress. HSPs are ubiquitous cellular proteins with a highly conserved structure, mode of regulation, and function, indicating their important role in cellular functions. HSPs are induced by physical and chemical insults, and confer

Table 5
Gene list of microarray

Spot	Gene name
A1	β prime COP
A2	adenylate kinase 1
A3	HLA-B-associated transcript 1A
A4	heat shock protein 90 (rats, brain, mRNA, 2524 nt)
A5	calnexin
A6	branched chain aminotransferase 1, cytosolic
A7	P450 (cytochrome) oxidoreductase
A8	X-ray repair cross-complementing group 1 protein
A9	carbonic anhydrase 2
B1	oxygen-regulated protein
B2	neogenin
B3	transferrin
B4	RPT protein similar to yeast MRS2
B5	adenylate kinase 4
B6	nuclear factor of κ light polypeptide gene enhancer in B cells inhibitor-like 1
B7	branched chain aminotransferase 2, mitochondrial
B8	metallothionein 1, pseudogene A
B9	RT1 class Ib gene, H2-TL-like, grc region (N1)
C1	glutathione S-transferase omega 1
C2	carbonic anhydrase 11
C3	thymus cell antigen 1, θ
C4	coatamer protein complex, subunit γ 1
C5	heat shock protein 60 (liver)
C6	tweety homolog 1 (Drosophila)
C7	excision repair cross-complementing rodent repair deficiency, complementation group 1
C8	calcium binding atopy-related autoantigen 1
C9	heat shock protein 8
D1	hemoglobin, α 1
D2	odd Oz/ten-m homolog 4 (Drosophila)
D3	DnaJ (Hsp40) homolog, subfamily B, member 5
D4	endoplasmic reticulum protein 29
D5	Nsf: N-ethylmaleimide sensitive factor
D6	esterase 10
D7	acyl-coA oxidase
D8	coatamer protein complex, subunit γ 2
D9	surfeit 1
E1	DnaJ-like protein
E2	glutathione S-transferase, μ type 3 (Yb3)
E3	activated leukocyte cell adhesion molecule
E4	α thalassemia/mental retardation syndrome X-linked homolog (human)
E5	GAPDH
E6	cleft lip and palate associated transmembrane protein 1
E7	heat shock 70 kDa protein 4
E8	heat shock 70 kDa protein 5
E9	peroxiredoxin 2
F1	cytochrome P450-like protein
F2	topoisomerase (DNA) III β
F3	thioredoxin domain containing 5
F4	superoxide dismutase 2
F5	negative control
F6	complement component factor h
F7	adenylate kinase 5
F8	similar to MHC class Ib RT1.S3
F9	limbic system-associated membrane protein
G1	epoxide hydrolase 1
G2	TAP binding protein
G3	Transthyretin (prealbumin, amyloidosis type I)
G4	hemoglobin β chain complex
G5	MHC class II-associated invariant chain
G6	glutathione S-transferase, μ 1

Table 5 (continued)

Spot	Gene name
G7	DnaJ (Hsp40) homolog, subfamily B, member 1
G8	cytochrome P450, subfamily 51
G9	immunoglobulin superfamily, member 8
H1	ferritin light chain 2
H2	glutathione transferase subunit 8
H3	mannose-binding protein associated serine protease-1
H4	NY-REN-18 antigen
H5	DnaJ (Hsp40) homolog, subfamily B, member 6
H6	T cell receptor γ locus, TCR γ 1 and γ 3 gene clusters
H7	coatamer protein complex, subunit β 1
H8	glutamate cysteine ligase, modifier subunit
H9	Sacm21/RT1-A intergenic region, haplotype RT1n and partial RT1-A gene for MHC class I antigen
I1	heat shock protein 1, α
I2	RAD50 homolog (<i>S. cerevisiae</i>)
I3	germline MHC class I gene, complete cds
I4	acyl-coenzyme A oxidase 3, pristanoyl
I5	β -2-microglobulin
I6	DnaJ (Hsp40) homolog, subfamily C, member 5
I7	non MHC restricted killing associated
I8	suppression of tumorigenicity 13 (colon carcinoma) Hsp70-interacting protein
I9	ferritin, heavy polypeptide 1
J1	creatine kinase, brain
J2	HLA-B-associated transcript 3
J3	thioredoxin-like 2
J4	B-cell receptor-associated protein 37
J5	selenium-dependent glutathione peroxidase mRNA, complete cds
J6	thioredoxin 2
J7	glycoprotein Ib (platelet), β polypeptide
J8	topoisomerase (DNA) II β
J9	HLA-B associated transcript 2
K1	islet cell autoantigen 1, 69 kDa
K2	heat shock factor binding protein 1
K3	stress-induced-phosphoprotein 1 (Hsp70/Hsp90-organizing protein)
K4	C4 complement protein
K5	18S rRNA
K6	thioredoxin domain containing 1
K7	platelet-activating factor acetylhydrolase α 2 subunit (PAF-AH α 2)
K8	coagulation factor C homolog (<i>Limulus polyphemus</i>)
K9	adenylate kinase 3
L1	glutathione S-transferase, θ 2
L2	RT1 class Ib gene (Aw2)
L3	proprotein convertase subtilisin/kexin type 3
L4	thioredoxin-like (32 kDa)
L5	blank
L6	glutathione S-transferase Yc1 subunit (rats, fetal liver, mRNA, 1052 nt)
L7	DnaJ (Hsp40) homolog, subfamily C, member 7
L8	ligase III, DNA, ATP-dependent
L9	SWI/SNF-related, matrix-associated, actin-dependent regulator of chromatin, subfamily e, member 1

cellular resistance to subsequent lethal stressors. For example, heat and ischemia are well known stimuli that induce the HSP70 family in the central nervous system [22]. In mammals, the HSP70 family is also stimulated by stress mediators such as adrenocorticotrophic hormone and catecholamines [3]. Accordingly, expression of the HSP70 family may be associated with stress responses involving

the endocrine, nervous, and immune systems. Glucocorticoid levels also are increased in depressed patients [4] and glucocorticoid receptor function is regulated by HSPs [23]. Thus, further investigation of the relationship between HSPs and psycho-physiological stress in hippocampus should be fruitful. In the present study, for example, we constructed a cDNA microarray focused on genes categorized into 'cell/organism defense', including a number of stress inducible factors such as HSPs, for further molecular studies in animal models of stress-related disorders.

As shown in Fig. 3 C, there was significant correlation between the frequencies of observed ESTs categorized into 'cell/organism defense' and the signal intensities of the spots, suggesting that the profiling of transcripts by ESTs reflects the actual gene expression pattern well. These clone sets allow for the production of large numbers of cDNA microarrays at low cost, permitting the use of large numbers of replicates in gene expression profiling experiments, which should lead to increased data quality. In addition, because many of the cDNAs spotted on our microarrays are not contained on commercial platforms at present, they should provide a unique and useful tool for molecular studies of animal models of stress-related disorders.

Functional analysis of newly discovered genes through this approach might clarify the molecular mechanisms underlying the pathogenesis of stress-related disorders sufficiently to reveal novel therapeutic targets. Integrated information on hippocampus-specific functions and mapping of our ESTs on the human chromosome should complement genetic linkage studies and facilitate positional candidate cloning for the identification of genes of memory-, learning- and stress-related disorders in genetically defined regions.

Acknowledgments

This study was supported by Grants-in-Aid for Scientific Research A-C and for Scientific Research on Priority Areas (C) "Medical Genome Science" from the Japanese Ministry of Science, Education, Sports, Culture and Technology; for a Health and Labor Science Research Grant for Special Research from the Japanese Ministry of Health, Labor and Welfare; and for the Yamanouchi Foundation for Research on Metabolic Disorders, Japan Diabetes Foundation and Takeda Science Foundation.

References

- [1] M.D. Adams, A.R. Kerlavage, R.D. Fleischmann, R.A. Fuldner, C.J. Bult, N.K. Lee, E.F. Kirkness, K.G. Weinstock, J.D. Gocayne, O. White, et al., Initial assessment of human gene diversity and expression patterns based upon 83 million nucleotides of cDNA sequence, *Nature* 377 (1995) 3–174 (Suppl.).
- [2] S.F. Altschul, T.L. Madden, A.A. Schäffer, J. Zhang, Z. Zhang, W. Miller, D.J. Lipman, Gapped BLAST and PSI-BLAST: a new generation of protein database search programs, *Nucleic Acids Res.* 25 (1997) 3389–3402.
- [3] M.J. Blake, D.J. Buckley, A.R. Buckley, Dopaminergic regulation of heat shock protein-70 expression in adrenal gland and aorta, *Endocrinology* 132 (1993) 1063–1070.
- [4] B.J. Carroll, The dexamethasone suppression test for melancholia, *Br. J. Psychiatry* 140 (1982) 292–304.
- [5] N.A. Datsun, J. van der Perk, E.R. de Kloet, E. Vreugdenhil, Expression profile of 30,000 genes in rat hippocampus using SAGE, *Hippocampus* 11 (2001) 430–444.
- [6] R.S. Duman, J. Malberg, J. Thome, Neural plasticity to stress and antidepressant treatment, *Biol. Psychiatry* 46 (1999) 1181–1191.
- [7] P.S. Eriksson, E. Perfilieva, T. Bjork-Eriksson, A.M. Alborn, C. Nordborg, D.A. Peterson, F.H. Gage, Neurogenesis in the adult human hippocampus, *Nat. Med.* 4 (1998) 1313–1317.
- [8] E. Fuchs, G. Flugge, Stress, glucocorticoids and structural plasticity of the hippocampus, *Neurosci. Biobehav. Rev.* 23 (1998) 295–300.
- [9] K. Fukunaga, L. Stoppini, E. Miyamoto, D. Muller, Long-term potentiation is associated with an increased activity of Ca^{2+} /calmodulin-dependent protein kinase II, *J. Biol. Chem.* 268 (1993) 7863–7867.
- [10] R.A. Gibbs, G.M. Weinstock, M.L. Metzker, D.M. Muzny, E.J. Sodergren, S. Scherer, G. Scott, D. Steffen, K.C. Worley, P.E. Burch, et al., Genome sequence of the Brown Norway rat yields insights into mammalian evolution, *Nature* 428 (2004) 493–521.
- [11] E. Gould, P. Tanapat, Stress and hippocampal neurogenesis, *Biol. Psychiatry* 46 (1999) 1472–1479.
- [12] J.P. Herman, M.K. Schafer, E.A. Young, R. Thompson, J. Douglass, H. Akil, S.J. Watson, Evidence for hippocampal regulation of neuroendocrine neurons of the hypothalamo-pituitary-adrenocortical axis, *J. Neurosci.* 9 (1989) 3072–3082.
- [13] D.M. Hwang, A.A. Dempsey, R.X. Wang, M. Rezvani, J.D. Barrans, et al., A genome-based resource for molecular cardiovascular medicine. Toward a compendium of cardiovascular genes, *Circulation* 96 (1997) 4146–4203.
- [14] T. Ichimura, T. Isobe, T. Okuyama, T. Yamauchi, H. Fujisawa, Brain 14-3-3 protein is an activator protein that activates tryptophan 5-monooxygenase and tyrosine 3-monooxygenase in the presence of Ca^{2+} , calmodulin-dependent protein kinase II, *FEBS Lett.* 13 (1987) 79–82.
- [15] L. Jin, H. Wang, T. Narita, R. Kikuno, O. Ohara, N. Shihara, T. Nishigori, Y. Horikawa, J. Takeda, Expression profile of mRNAs from human pancreatic islet tumors, *J. Mol. Endocrinol.* 31 (2003) 519–528.
- [16] E.R. Kandel, The molecular biology of memory storage: a dialogue between genes and synapses, *Science* 294 (2001) 1030–1038.
- [17] E.H. Margulies, S.L.R. Kardia, J.W. Innis, Identification and prevention of a GC content bias in SAGE libraries, *Nucleic Acids Res.* 29 (12) (2001) E60-0.
- [18] A. Matynia, S.G. Angnostaras, A.J. Silva, Weaving the molecular and cognitive strands of memory, *Neuron* 32 (2001) 557–559.
- [19] M. Mayford, J. Wang, E. Kandel, T.S. O'Dell, CAMK II regulates the frequency-response function of hippocampal synapses for the production of both LTD and LTP, *Cell* 81 (1995) 891–904.
- [20] B.S. McEwen, The neurobiology of stress: from serendipity to clinical relevance, *Brain Res.* 886 (2000) 172–189.
- [21] M. Nilsson, E. Perfilieva, U. Johansson, O. Orwar, P.S. Eriksson, Enriched environment increases neurogenesis in the adult rat dentate gyrus and improves spatial memory, *J. Neurobiol.* 39 (1999) 569–578.
- [22] T.S. Nowak Jr., U. Bond, M.J. Schlesinger, Heat shock RNA levels in brain and other tissues after hyperthermia and transient ischemia, *J. Neurochem.* 54 (1990) 451–458.
- [23] W.B. Pratt, D.O. Tort, Steroid receptor interactions with heat shock protein and immunophilin chaperones, *Endocr. Rev.* 18 (1997) 306–360.
- [24] R.M. Sapolsky, Glucocorticoids and hippocampal atrophy in neuropsychiatric disorders, *Arch. Gen. Psychiatry* 57 (2000) 925–935.